# RUNAWAY ESCAPEMENT REDESIGN M125A1 MODULAR BOOSTER

Louis P. Farace

Frankford Arsenal
Philadelphia, Pennsylvania

December 1974

## DISPOSITION

Destroy this report when it is no longer needed. Do not return it to the originator.

Citation of manufacturer s names in this report does not constitute an official indorsement of the use of such commercial hardware or software.

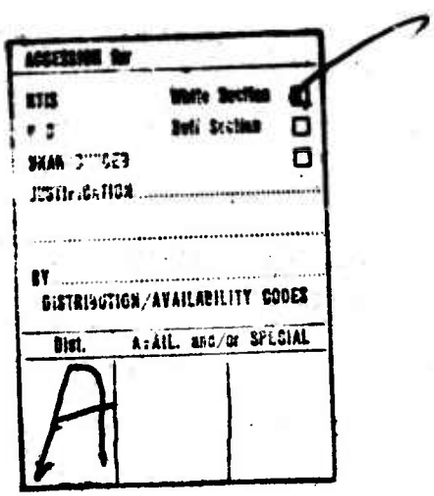


The findings in this report are not to be construed as an official Department of the Army position, unless so designated by other authorized documents.

UNCLASSIFIED

SECURITY CLASSIFICATION OF THIS PAGE (When Data Entered)

| REPORT DOCUMENTATION PAGE | | READ INSTRUCTIONS BEFORE COMPLETING FORM |
|---|---|---|
| 1. REPORT NUMBER<br>FA-TR-74045 | 2. GOVT ACCESSION NO. | 3. RECIPIENT'S CATALOG NUMBER<br>AD-A009 723 |
| 4. TITLE (and Subtitle)<br>RUNAWAY ESCAPEMENT REDESIGN M125A1 MODULAR BOOSTER | | 5. TYPE OF REPORT & PERIOD COVERED<br>Technical research report<br>6. PERFORMING ORG. REPORT NUMBER |
| 7. AUTHOR(s)<br>LOUIS P. FARACE | | 8. CONTRACT OR GRANT NUMBER(s) |
| 9. PERFORMING ORGANIZATION NAME AND ADDRESS<br>Frankford Arsenal<br>Attn: SARFA-MDA-E<br>Philadelphia, PA 19137 | | 10. PROGRAM ELEMENT, PROJECT, TASK AREA & WORK UNIT NUMBERS<br>AMCMS: 4110.16.4737.6 |
| 11. CONTROLLING OFFICE NAME AND ADDRESS<br>ARMCOM | | 12. REPORT DATE<br>December 1974<br>13. NUMBER OF PAGES<br>60 |
| 14. MONITORING AGENCY NAME & ADDRESS(if different from Controlling Office) | | 15. SECURITY CLASS. (of this report)<br>UNCLASSIFIED<br>15a. DECLASSIFICATION/DOWNGRADING SCHEDULE<br>N/A |

16. DISTRIBUTION STATEMENT (of this Report)

Approved for public release; distribution unlimited.

17. DISTRIBUTION STATEMENT (of the abstract entered in Block 20, if different from Report)

18. SUPPLEMENTARY NOTES



19. KEY WORDS (Continue on reverse side if necessary and identify by block number)

M125A1 Booster
Delay Arming Mechanism
Runaway Escapement
Math Model
Gear Mesh
Pivot Friction
Journal Bearing Losses

20. ABSTRACT (Continue on reverse side if necessary and identify by block number)

An analytical investigation was conducted to determine the effect of friction on the modular version of the M125A1 Booster mechanism, a Safe and Arming Device which operates in a centrifugal force field created by a spinning projectile. The investigation uncovered two points of contact which were extremely sensitive to friction.

Cont'd

DD FORM 1 JAN 73 1473 EDITION OF 1 NOV 65 IS OBSOLETE

PRICES SUBJECT TO CHANGE

UNCLASSIFIED

SECURITY CLASSIFICATION OF THIS PAGE (When Data Entered)

20. ABSTRACT - Cont'd

Subsequent redesign utilizing a simple friction loss math model and a computer program to analyze the escapement mesh resulted in a design which operated significantly smoother and started more readily. Both laboratory and ballistic tests verified that this new version met all timing and functioning requirements with a high degree of accuracy and reliability. It is anticipated that production of the new design in mass quantities will result in increased production yield and improved performance with no increase in cost.

## TABLE OF CONTENTS

TABLE OF CONTENTS - Cont'd



List of Illustrations

List of Tables

# GLOSSARY

| | | |
|---|---|---|
| $a$ | = | thrust acceleration of particular environment |
| $A_p$ | = | input moment arm of force |
| $A'_p$ | = | friction modified input moment arm of force |
| $A_w$ | = | output moment arm of force |
| $A'_w$ | = | friction modified output moment arm of force |
| $E$ | = | system efficiency |
| $E_p$ | = | escapement mesh efficiency |
| $F$ | = | FORCE |
| $\vec{F}$ | = | vector sum of $\vec{F}$ and $\mu \vec{F}$ |
| $g_1$ | = | bearing losses (total) in stage 1 |
| $g_2$ | = | bearing losses (total) in stage 2 |
| $g_j$ | = | bearing losses (total) in stage j |
| $g_s$ | = | bearing losses due to sideloads |
| $g_t$ | = | bearing losses due to thrust loads |
| $G_{p.lev}$ | = | torque transmitted to pallet lever |
| $G_{s.whl}$ | = | net torque output of escapewheel |
| $I_1$ | = | inertia of gear/wheel 1 |
| $I_2$ | = | inertia of gear/wheel 2 |
| $I_j$ | = | inertia of gear/wheel j |
| $m_{p.L}$ | = | mass of pallet lever |
| $M_1$ | = | input moment on gear/wheel 1 |

## GLOSSARY (Cont'd)

| | | |
|---|---|---|
| $M_2$ | = | input moment on gear/wheel 2 |
| $P$ | = | load |
| $P_t$ | = | thrust load |
| $R_1^*$ | = | $A_w^*$ |
| $R_2$ | = | $A_p^*$ |
| $R_i$ | = | inner radius of collar bearing |
| $R_o$ | = | outer radius of collar bearing |
| $\vec{R}_p$ | = | position vector locating contact point relative to lever's pivot |
| $R_{p,L}$ | = | pivot location offset from mechanism spin center |
| $\vec{R}_w$ | = | position vector locating contact point relative to escapewheel pivot |
| $\alpha$ | = | included angle between line of action and normal to $R_w$ |
| $\eta$ | = | gear ratio |
| $\eta^*$ | = | torque ratio |
| $\eta_{21}$ | = | gear ratio between gears 2 and 1. |
| $\eta_{21}^*$ | = | torque ratio between gears 2 and 1 |
| $\eta_{ij}$ | = | gear ratio between gears i and j |
| $\eta_p$ | = | linkage ratio |
| $\eta_p^*$ | = | escapement torque ratio |

## GLOSSARY (Cont'd)

$\ddot{\theta}_1$ = angular acceleration of gear/wheel 1

$\ddot{\theta}_2$ = angular acceleration of gear/wheel 2

$\lambda$ = escapewheel half angle

$\mu$ = coefficient of friction

$\xi$ = tau$^{-1}$ $\mu$

$\rho_p$ = journal radius

$\rho_{p.l.}$ = journal radius of pallet pivot

$\tau$ = included angle between line of action and $R_p$

$\omega$ = angular velocity of projectile

## INTRODUCTION

This report first supplies general information relevant to the nature of the M125A1 Booster and its application. Secondly, the escapement changes made are described along with test results obtained with the redesigned escapement. Thirdly, the math model and analytical formulations which motivated these design changes are presented. Finally a discussion of the parameters in the math model is presented along with evaluation of these parameters where possible.

Two friction sensitive areas were identified by the math model as being more important than most -- the escapewheel pin pallet mesh point, and the journal bearing contacts of the pallet lever. Both are contained in the escapement portion of the mechanism. Hence, design changes were made to reduce the frictional torque in this area. Appropriate action has been taken to incorporate these changes into the M125A1 Booster Technical Data Package (TDP).

## GENERAL INFORMATION

The modular DAM Part #11743960 is the Safe and Arming device used in the M557 and M564/M565 Alternate (Alt) fuzes. For use in M557 fuze, the module is housed in an aluminum body, the resulting combination of which is presently referred to as the M125A1 Booster (Figure 1). This booster is then threaded onto the base of this fuze for use on cannon launched spin stabilized projectiles. For use in the M564 and M565 Alt fuzes, the module is housed in a smaller aluminum housing which is threaded into the base of the fuze.

The function of the DAM is to delay arming of the fuze until the projectile is a safe distance from the weapon. This time delay is provided by a combination of two factors: the number of oscillation cycles of the escapement before the out-of-line detonator becomes aligned, and the frequency at which these oscillations are taking place. The ratio of these two factors yields the time delay of the mechanism.

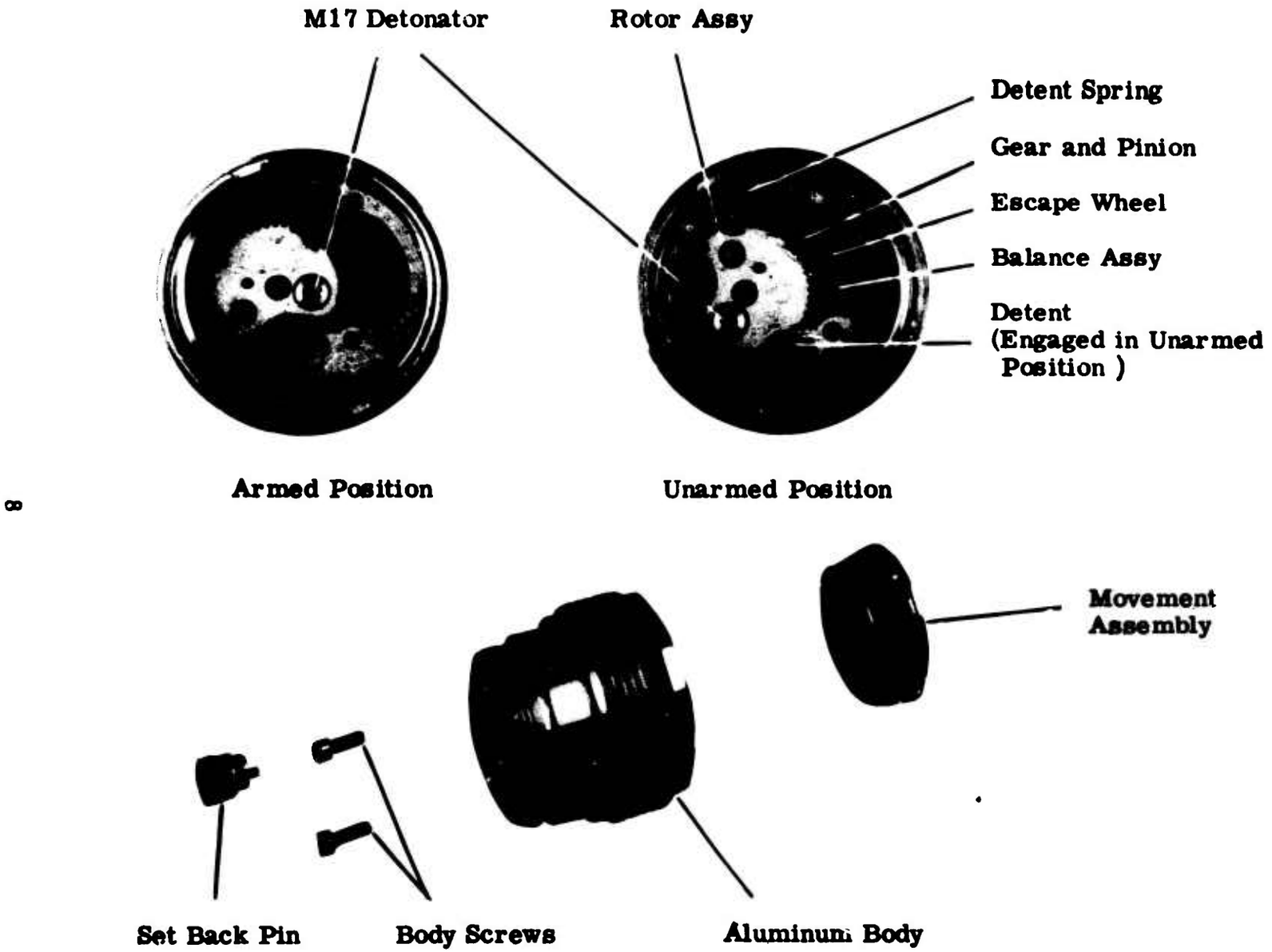


Figure 1. M125A1 Modular Booster

The first factor (quantity of cycles) is built into the design by virtue of the number of teeth on the escapewheel, the gear ratio between the escapewheel and the gear carrying the out-of-line detonator, and the angular travel of the detonator-carrying gear (rotor gear) required for alignment. The second factor (rate of cycling) is a function of projectile spin rate and numerous other factors inherent in the mechanism. The projectile spin not only powers the centrifugal rotor gear which ultimately drives the mechanism, but produces radial loads on all mechanism components as well.

The mechanism is required to operate at a spin level of 2000 rpm but contains safety detents which must prevent operation below 1000 rpm. This does not preclude, however, the possibility of the mechanism being operable below the 1000 rpm spin level when the spin detents are removed.

The ability of the mechanism to start and sustain operation at a given spin level is largely dependent upon the amount of frictional torque present in the mechanism relative to the output torque of the centrifugal gear at that spin level. Improving starting capability can be accomplished by either minimizing the friction in the device, desensitizing the mechanism to withstand that level of friction which does exist (increase the overall efficiency), or supplying more input torque.

This report focuses on the first two alternatives and then illustrates how a redesign technique was employed in improving the starting capability of the M125A1 Modular Booster. Test results and general information concerning this redesigned mechanism are given first followed by the analysis.

## ESCAPEMENT REDESIGN DESCRIPTION

The redesign consisted of the following:

a. Replacing the escapement configuration with that configuration utilized in the M125A1 Alt (Non-Modular version) booster insofar as pallet pin size and position, escapewheel radius and tooth angle, and center-to-center distance between escapewheel and pallet lever.

b. Utilizing a high-inertia lightweight pallet lever configuration.

c. Reducing the outer radius of the lower bearing of the pallet lever.

d. Moving the pallet pivot closer to the spin axis.

Figure 2 illustrates the original and the improved escapement configurations respectively. In general, a runaway escapement configuration can be described using nine parameters. Each are listed in the table below with appropriate dimensions for both configurations.

TABLE I.
Comparison of Escapement Dimensions

| Parameters | Dimensions | |
|---|---|---|
| | Original | Improved |
| Pallet Pin Radius | .01275 in. | .015 in. |
| Included Angle btw Pin Pallets | 103°47' | 152°06' |
| Radial Location of Pin Pallets | .1426 in. | .0788 in. |
| Escapement Center-to-Center Distance | .2331 in. | .2035 in. |
| Escapewheel radius | .1855 in. | .192 in. |
| Escapewheel tooth angle | 27°30' | 51° |
| Number of Escapewheel Teeth | 12. | 12. |
| Blend Radius at Tooth Tip | .003 in. | .003 in. |
| Number of Teeth Spanned by Pin Pallets | 2.5 | 1.5 |

The improved dimensions are those used on the Non-Modular M125A1 Alt Booster. Over 150 million boosters with this escapement have been produced since 1966. These dimensions originated with the Ingraham Watch Co. through a Product Improvement Contract in which various aspects of producibility were addressed. This design provides adequate escapement clearances and can be shown to be very efficient insofar as transmitting torque from the escapewheel to the pallet lever in the presence of coulomb friction. In general, with this escapement, more torque is transmitted to the pallet lever than with the original Modular M125A1 escapement. This alone is beneficial in the sense that more torque now becomes available to overcome the frictional torque in the pallet lever's bearings. However, this also causes the lever to oscillate faster unless its polar moment of inertia is adjusted accordingly.

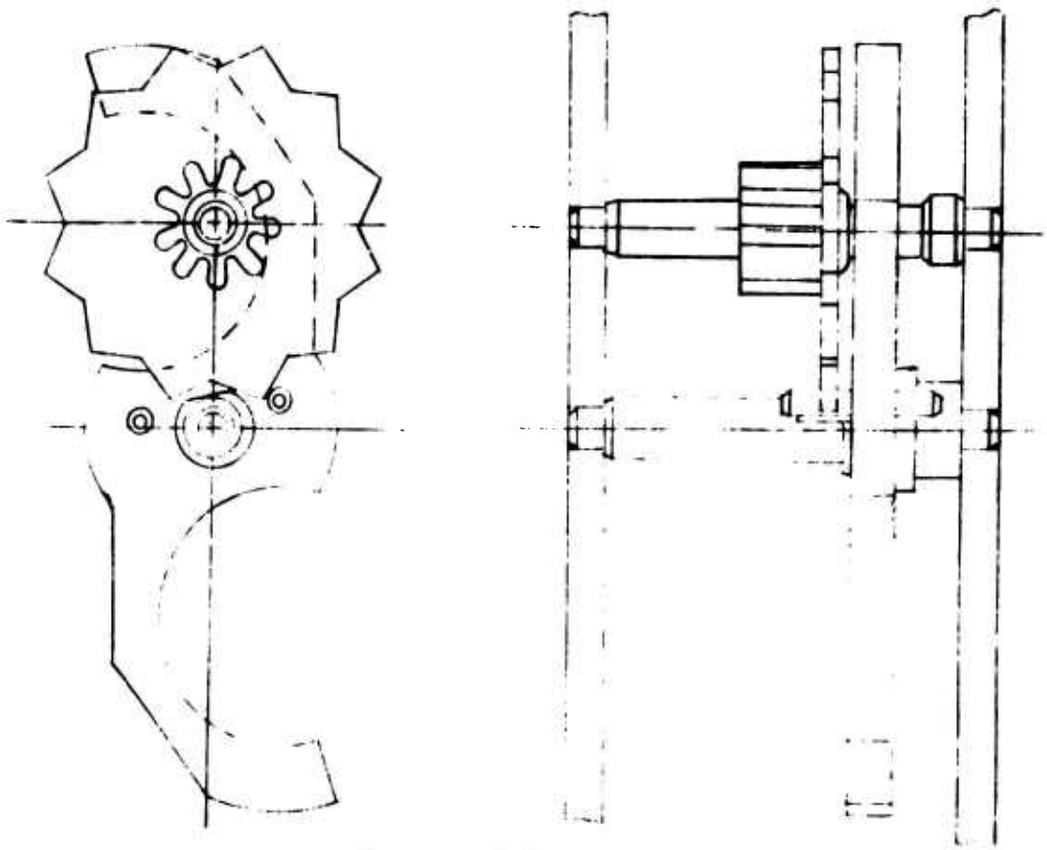

Improved Escapement

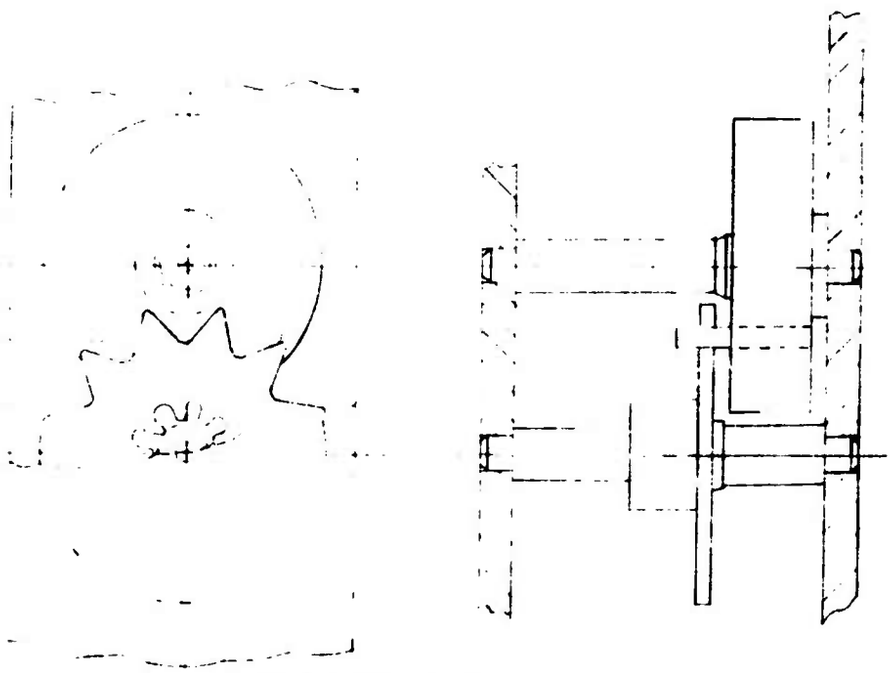

Original Escapement

Figure 2. M125A1 Modular Booster Escapements

The improved lever differs significantly from the original lever. It is lighter, thinner, and higher in inertia. It is shaped such that the arms fit around and partially encircle the escapewheel pivot. The extended arms produce a large radius of gyration providing more inertia through the use of less mass. This is beneficial in two respects: 1) it compensates the timing alteration induced by the higher torque escapement configuration; and 2) it reduces the frictional torque in the bearings of the pallet lever. This lever configuration is 40 percent lighter in weight and 75 percent higher in inertia. In addition, the position of the pallet lever relative to the spin center of the booster was changed bringing it closer to the spin center to further reduce the magnitude of the centrifugal force acting on the lever. Also, the diameter of the thrust bearing of the pallet lever was reduced. The lighter weight combined with the reduction in bearing diameter and off-center position serve to decrease the frictional torque at the pallet lever by more than half. Table I lists dimensions and parameters contrasting the two pallet lever configurations.

It can be seen that the sum total of escapement changes serve to reduce the frictional torque in the pallet lever's bearings, and increase the torque transmitted to the lever from the escapewheel. This was done without decreasing the arming time. Test results on the prototypes of this improved escapement indicated that low spin performance of the mechanism was greatly improved as was expected. An engineering order was subsequently issued to implement these design changes into the Technical Data Package following approval by Frankford Arsenal's Fuze Configuration Control Board. All tests performed during the program will be discussed herein.

## CHARACTERISTICS OF THE M125A1 MODULAR BOOSTER

The time delay mechanism in the modular M125A1 Booster consists of a centrifugal gear, one gear and pinion assembly, and a runaway escapement. This escapement is composed of two parts, an escapewheel and a pin pallet lever. The non-modular version of the M125A1 Booster contained the same components with the exception that it contained one additional gear and pinion assembly. It was demonstrated

both empirically and analytically that the non-modular M125A1 (now referred to the M125A1 Alt) was a turns-counting mechanism. It was armed in the same number of turns regardless of the angular speed at which it made those turns. It was demonstrated analytically that this turns-counting characteristic arises whenever a centrifugal gear is used to power a runaway escapement. The present M125A1 Alt has been shown to arm in about 39 turns; however the M125A1 modular booster arms in approximately 30 turns, the decrease in turns being due mostly to the absence of the additional gear stage. Frankford Arsenal technical report R-2006* shows how this constant turns-to-arm is very useful since it establishes for a given weapon a fixed distance-to-arm which is not related to spin speed or propellant charge level.

The turns-to-arm vs angular velocity curve has been observed to take the general form of Figure 3.

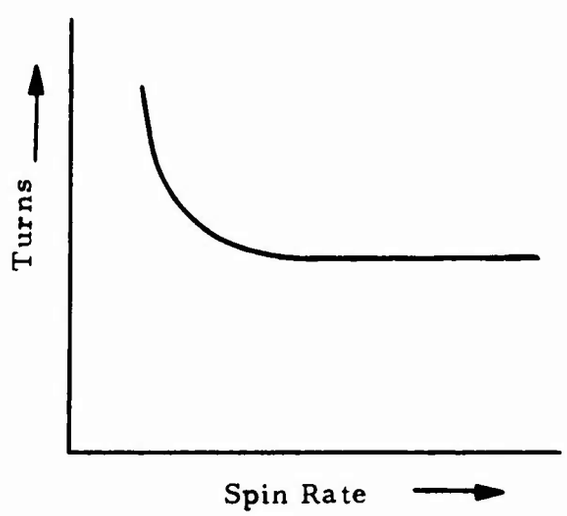


Figure 3. Turns-to-Arm vs Booster Angular Velocity

* Louis P. Farace and Seth D. Shapiro, "Computer Approximation for the Runaway Escapement in Varying Torque Environments: M125A1-M125A1E3 Booster," Frankford Arsenal Report R-2006, May 1971.

The constant turns-to-arm characteristic holds for the flat portion of the curve and contains that range of rpm experienced ballistically (2,750 thru 19,500 rpm). The early slope of the curve arises from the effect of spin invariant frictional losses such as the gravitational axial load of the rotor and gear members on their respective bearing surfaces. In contrast, the side thrust loading is spin dependent since it arises from centrifugal force and varies as the square of the angular velocity. Thus at very low rpm. (below 1000), the spin invariant frictional losses can be comparable to spin dependent frictional losses and result in a net torque which is not directly proportional to the square of the angular velocity. As the angular velocity increases, however, these spin invariant frictional losses and the net drive torque becomes approximately proportional to the square of the angular velocity.

Observe from Figure 3 that there is some cutoff rpm below which the mechanism will not run. This threshold value is affected by many factors including the basic design of the mechanism, the surface finishes at all contact points, the degree of lubrication at these points, and the angular acceleration by which the booster reaches this rpm. A high angular acceleration induces dynamic effects into the mechanism which generally lower the threshold rpm. Conversely, a low angular acceleration may not induce dynamic effects and this increases the threshold rpm value. Since the booster is required to be operative at 2000 rpm, it is felt that the lower the threshold rpm level, the greater the margin of excess torque available to pass the 2000 rpm spin test. It was found possible to significantly decrease these losses by introducing into the DAM design a higher inertia - lighter weight balance and a higher torque escapement. It will be shown how this combination significantly decreased the threshold rpm, thereby, increasing the excess torque margin at low spin levels.

## TEST RESULTS

Three versions of Higher-Inertia Lighter Weight pallet levers were tested ballistically. All versions met ballistic requirements although exhibiting somewhat different arming patterns insofar as 50 percent or mean arming distance. Test results for the final design implemented into the TDP will be given first.

## 1. FINAL DESIGN

### A. Ballistic Test Results

All tests were performed at ambient temperature using M48A3 fuzes set SQ.

| Weapon | Zone-Charge | Type Test | Rds Fired | Remarks |
|---|---|---|---|---|
| 90 mm M41 Gun | Service | Recovery | 30 | No structural damage observed in escapement area. |
| 90 mm M41 Gun | Service | Bruceton Arming Distance Test | 30 | Mean 233.6 ft-31.7 turns Std dev 3 ft - .4 turns |
| 8 inch Gun Howitzer | Z1 | Ground Impact | 40 | No duds |
| 155 mm Howitzer | Z1 | Ground Impact | 40 | No duds |
| 105 mm Howitzer M103 | Z7 | Ground Impact | 40 | No duds |
| 175 mm Howitzer | Z3 | Ground Impact | 40 | No duds |

These ballistic tests were designed to represent the extremes of spin environments to which the DAM might be exposed in field usage. The 90 mm gun produces a spin environment of approximately 19,500 rpm, the highest of all the weapons for which this booster is used. The 175 mm gun Z3 produces a spin of 15,700 rpm as does the 105 mm Howitzer M103 Z7. For low rpm the 8 inch Howitzer, Z1 produces a spin of 2950 rpm while the 155mm Howitzer, Z1 yields 3210 rpm. These weapons also span the range of setback environments in question. Recovery tests indicated no visible deformation of the pallet lever nor was there any distortion of the balance pins. Neither was any unusual coining of the movement plate observed at the balance pivot where the reduced diameter thrust bearing was used.

## B. Laboratory Tests

1. A random sample of ten units was taken prior to ballistic testing. All units were capable of arming at 1000 rpm with spinner motor controls set to produce a slow risetime in an effort to minimize dynamic effects. All units were lubricated with standard MIL-L-11734 fuze oil. No dry film lubricants were used or found necessary during any testing performed throughout this study.

Low rpm spin tests performed on previous models similar to the final design were not duplicated since it was felt that the designs were nearly indentical insofar as properties affecting starting capability. See Frankford Arsenal technical report R-2070* for a discussion of low spin laboratory testing and how it can be used as a tool in determining important system parameters on a comparative basis.

2. The remaining units fabricated for ballistic testing were spun at 2000 rpm. All units armed without any hesitation. Motor controls were set to produce a slow risetime.

3. Data was also collected insofar as the sensitivity of the new design to eccentric spin. In general, however, eccentric spin can produce both more and less rotor torque at a given rpm than will concentric spin. Orientation of the mechanism relative to the true spin center of the device becomes important here since centrifugal loading on all gear members including the rotor changes in magnitude and direction relative to the geometric center of the device. Thus testing is preferred in as many orientations as possible for a given ecentricity. Five units were tested to determine the maximum eccentricity at which the DAM could arm in all orientations (8 equally spaced orientations actually tested). Since the test fixture was capable of producing eccentricities in increments of .015 inches, only bounds could be placed on the test results. This test was conducted at 2000 rpm.

---

Louis P. Farace and James P. Harper, " Feasibility of Dry Film Lubrication for the M125A1 Booster, " Frankford Arsenal Report R-2070, March 1973.

| Unit No. | Radial Eccentric Spin Capability (RESC) |
|---|---|
| 1 | .075 < RESC < .090 |
| 2 | .060 < RESC < .075 |
| 3 | .075 < RESC < .090 |
| 4 | .060 < RESC < .075 |
| 5 | .075 < RESC < .090 |

## 2. PROTOTYPE DESIGN

Figure 4 depicts the initial prototypes of the High-Inertia Lightweight Pallet lever plus high torque escapement. It was designed to resemble a pallet lever used in an experiment conducted by David Overman of Harry Diamond Laboratories This lever, when placed in a specially modified M125A1 Alt booster (non-modular) increased the arming time from approximately 40 turns to over 100 turns.

Design alterations were made to fit the lever depicted in Figure 4 into the module under the escapewheel. The design which resulted was fabricated out of strip stock and required a substantial amount of milling operations - undesirable from a mass production viewpoint but satisfactory for prototype testing to verify predictions of the math model. Following are test results obtained with this design:

### A. Ballistic Test Results

All tests were performed at ambient temperature using M48A3 fuzes set SQ.

| Weapon | Zone-Charge | Type Test | Rds Fired | Remarks |
|---|---|---|---|---|
| 75 mm AA Gun | Service | Recovery | 10 | Pallet pins found bent and worn |
| 105 mm Howitzer M2A1 | 7 | Bruceton Arming Distance Test | | Mean 197.54 ft-28.6 turns Std dev 3.5 ft-.5 turns |
| 155 mm Howitzer | 1 | Ground Impact | 30 | No duds |

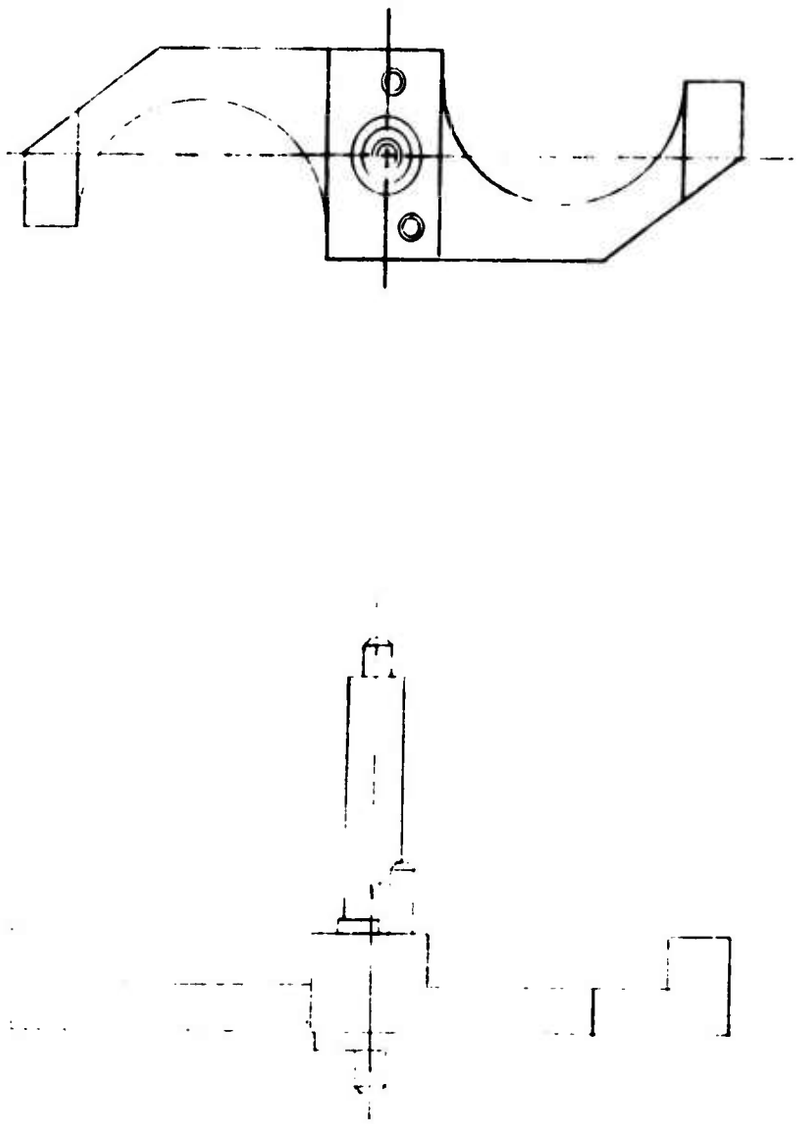

Figure 4. Prototype Lever Configuration

Comments:

1. Subsequent testing indicated that the pallet pins had not been hardened to the RC 38-42 required but were approximately RC 20. In addition, the 27,000 rpm - 21,000 g environment of the 75 mm AA gun also produced visible damage to a group of control boosters (modular M125A1) in the same fashion. The pins in this booster were hardened properly. The spin environment produced by this weapon generates forces twice as high as that of the 90 mm M41 gun, the highest spin weapon now used. Thus the recovery test was a severe overtest.

2. The soft balance pins could have produced a lower mean arming distance than that indicative of the device. The soft pin material would tend to wear away under high loading producing a different "effective" escapement geometry. Even so the arming time produced was only slightly faster than a group of standard M125A1 modular boosters fired from the same weapon at the same time. The mean arming distance for this group was 200 feet (29.0 turns).

## B. Laboratory Tests

1. Start up spin tests were performed on 100 units made to this design to determine the threshold functioning rpm. In each case the spin speed was slowly increased from rest to that rpm at which the mechanism began to operate. This eliminates any dynamic effects induced by high angular acceleration of the mechanism. The average threshold rpm was 1028.7 with a lowest measurement of 880 rpm and a high of 1180 rpm.

2. Turns-to-arm spin tests at 3000 rpm on 100 units yielded a mean of 34.04 turns. This tends to support the hypothesis that the 28.6 turns experienced ballistically was lower than that indicative of the device due to the soft pallet pins inadvertently utilized.

3. Turns-to-arm versus spin speed tests were performed using nine of the 100 units fabricated. Figure 5 indicates the results. These measurements were taken with a different test rig than that used in the previous test. It has been observed that this second test apparatus generally yields approximately 2 turns lower than the first. Observe that the spread of test data tightens with increased spin rate.

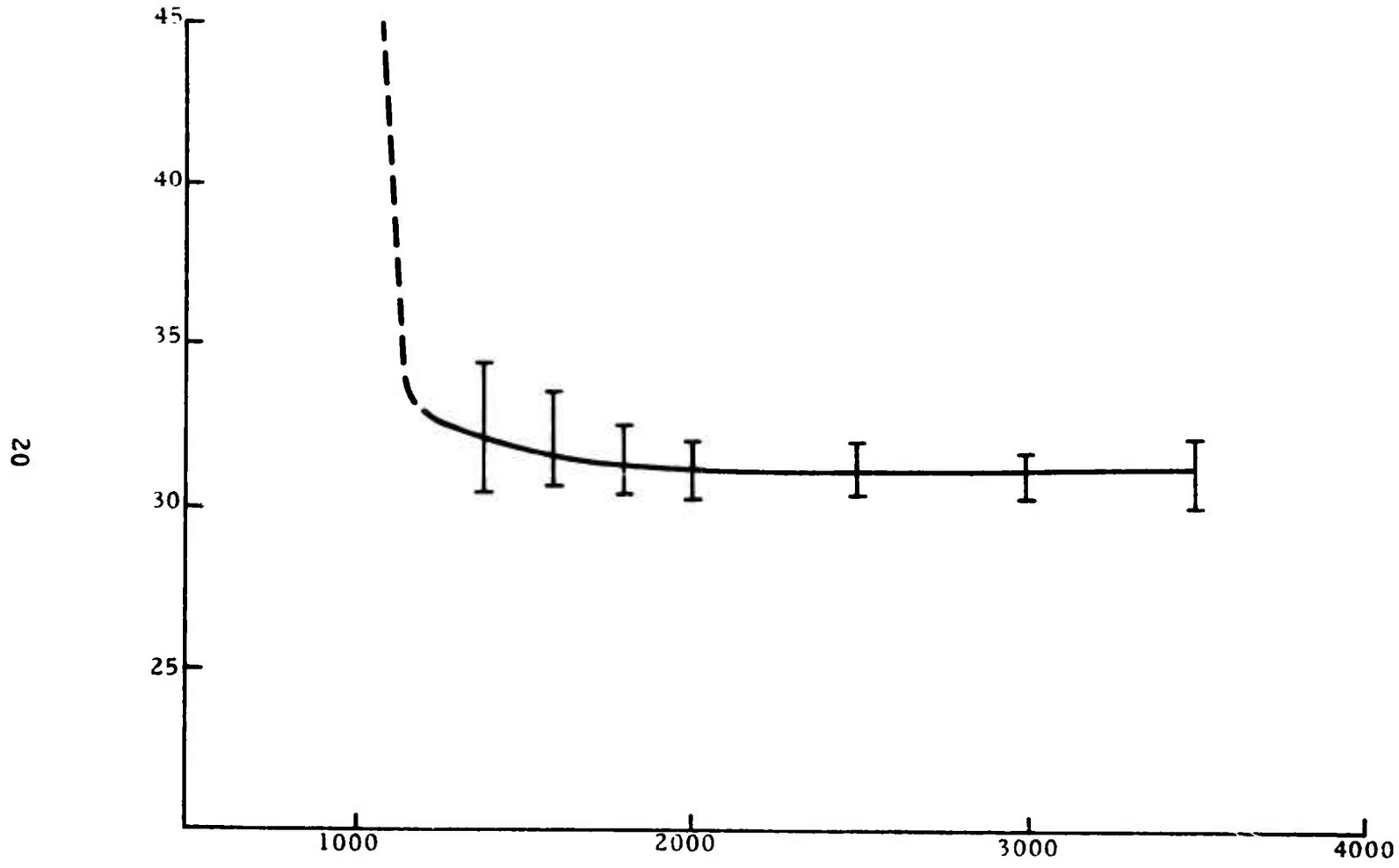


Figure 5. Turns-to-Arm vs Angular Velocity: Prototype Lever Configuration

It was apparent from the performance of these prototypes that the combination of high inertia balance and high torque escapement significantly improved the low spin performance of the device and could, therefore, be expected to increase the reliability of the mechanism and decrease the production scrap rate resulting from fallout in the 2000 rpm acceptance spin test. Production of the modular booster at this time had been limited to small lots (5000 max) and it was evident that that design could perform reliably but required more care and closer quality control than would be desirable in mass production; otherwise a high fallout rate might result.

## 3. INTERIM DESIGN

An effort was made at this point to develop a high inertia-high torque escapement resembling the prototypes as closely as possible but with an eye toward producibility using standard mass production techniques. The design which evolved is depicted in Figure 6. This lever was formed from half hard brass strip. Subsequent milling was performed for the test quantity fabricated, but it was felt that the end item could be produced inexpensively using progressive die forming operations. This lever assembly was slightly lighter than the prototypes and was lower in inertia, mainly because the formed-up material at the ends of the lever were constrained to be the thickness of the strip stock.

A quantity of 500 units was fabricated and tested as follows:

### A. Ballistic Tests

| Weapon | Zone-Charge | Type Test | Rds Fired | Remarks |
|---|---|---|---|---|
| 90 mm Gun M41 | Service | Ground Impact | 40 | No duds |
| 105 mm Howitzer M103 | 7 | Ground Impact | 40 | No duds |
| 8 inch Howitzer | 1 | Ground Impact | 40 | No duds |
| 155 mm Howitzer | 1 | Ground Impact | 40 | No duds |
| 90 mm M41 Gun | Service | Bruceton Arming Distance Test | 30 | Mean 162.4 ft 26.18 turns<br>Std dev 6.9 ft .93 turns |

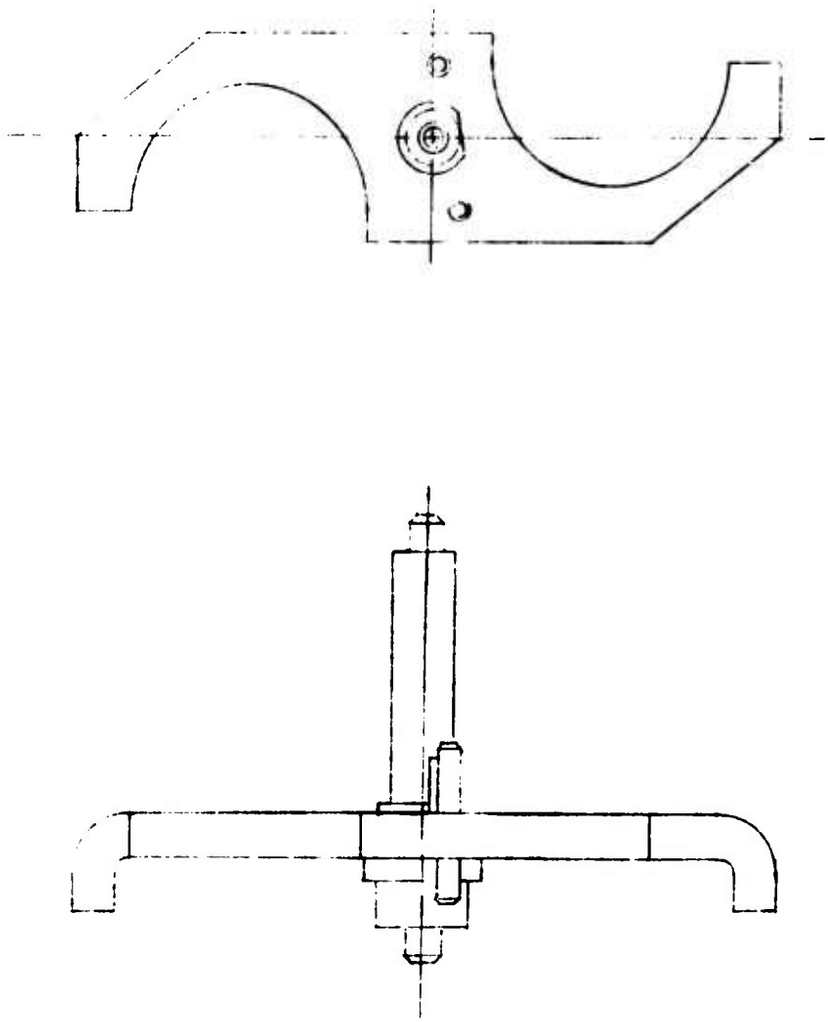

Figure 6. "Formed" Lever Configuration

## B. Rough Handling Tests

The following tests were run in accordance with MIL-STD-331A.

| Test | Units Tested | Results |
|---|---|---|
| Jumble | 32 | No failures |
| Jolt | 32 | No failures |
| Transportation/Vibration | 32 | No failures |
| Five Foot Drop | 25 | No failures |
| Forty Foot Drop | 25 | No failures |

## C. Laboratory Tests

1. Turns-to-arm measurements taken on 120 units at 2600 rpm yielded a mean of 33.78 turns with a standard deviation of 1.06 turns. The drop of over 7 turns from spin tests to ballistics cannot be explained. The most probable explanation may be a baseline shift on the laboratory turns measuring equipment. In general, Frankford's data indicates that lower arming turns result when units are tested ballistically. Pallet pins in these units were hardened properly so pin wear can be discounted as a possibility. Similarly pin distortion can be discounted since it was not observed in recovered 90 mm units in which the fuze malfunctioned but the S&A armed. Non-permanent deflection of the pins could explain the drop but no effort was directed toward verifying this hypothesis since the mean figure of 26.18 turns was considered acceptable.

2. Turns-to-arm vs spin speed tests were conducted on ten units. The results are depicted in Figure 7. These units appeared slightly more capable of functioning at 1000 rpm than the prototypes - possibly because the levers were slightly lighter.

3. Threshold starting rpm was measured for these same ten units. Mean threshold rpm was measured to be 839 rpm with a measured max of 880 rpm and min of 750 rpm. In contrast with the prototypes, the lower threshold rpm could be explained again by the small difference in lever weight and the sample sizes involved (10 tested with this design vs 100 of the prototypes).

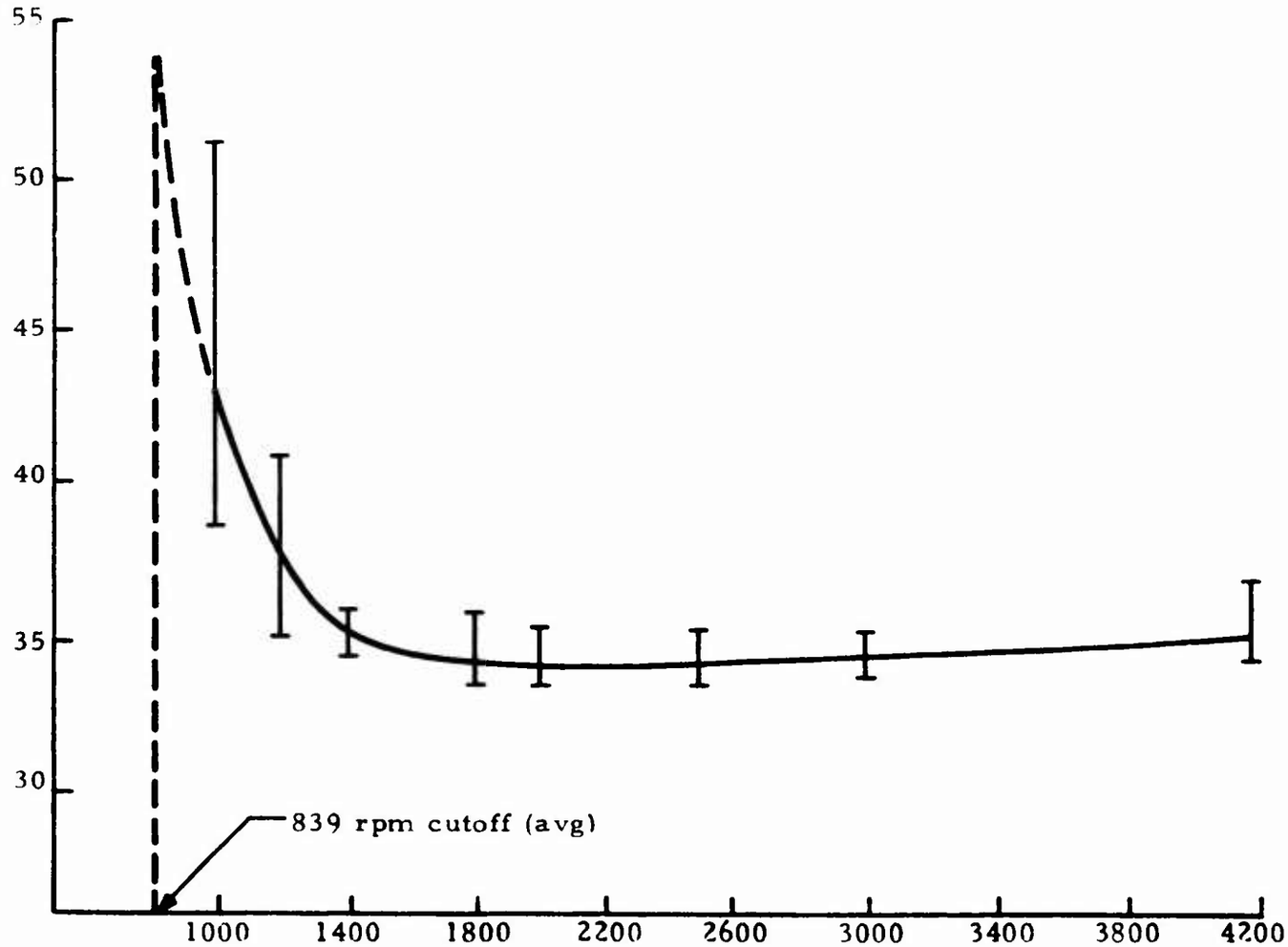


Figure 7. Turns-to-Arm vs Spin Rate: "Formed Lever"

## GENERAL COMMENTS

Efforts were undertaken at this time to incorporate the formed high inertia-high torque escapement into the TDP. A contract had already been placed for a large quantity of Modular M125A1 Boosters and also the DAM - the module part of this booster. Cost estimates to incorporate the new escapement into these contracts was estimated to be over $50,000 - partially due to the cost of the new lever. While it was intended that the lever be a progressive form and die part, the contractor and his vendors maintained that milling operations would still be required unless fine blanking techniques were utilized. At this point, EO action was suspended and further design efforts were directed toward developing a lever of constant thickness which could be stamped routinely and thus be less expensive.

This resulted in the design depicted in Figure 8. In effect, the material previously formed up at the end of the lever was folded out and shaped. Material was added around the exit pallet pin hole to permit the pin holes to be pierced - eliminating secondary drilling operations. Material was added diagonally opposite this area to maintain symmetry. The added weight was compensated for by reducing the thrust bearing diameter of the pallet shaft - a factor which the friction loss math model predicted would decrease non spin dependent frictional drag in the lever's bearings. What resulted was a lever higher in inertia than the formed lever and approximately the same weight as the previous prototype lever. A quantity of units were fabricated for further testing. Results were reported previously. This design was eventually EO'd into the TDP at no additional cost on a non-obsolescence basis.

## FRICTION LOSS MATH MODEL

The following analysis assumes that the motion of a system controlled by a runaway escapement can be described as if it were a system of inertia wheels to which an additional stage is added periodically at the high speed end of the gear train. In addition, the system is assumed to stop when the additional stage is added corresponding to the impact between the escapewheel and pallet lever. This approach was initially used to approximate the arming time of

HIGH INERTIA PALLET LEVER

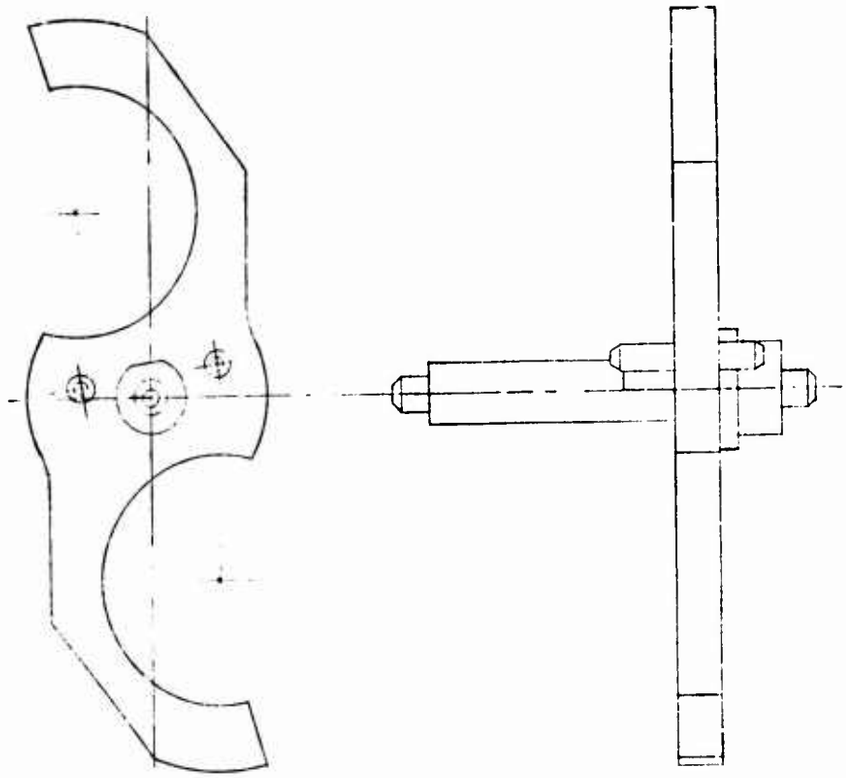

STANDARD PALLET LEVER

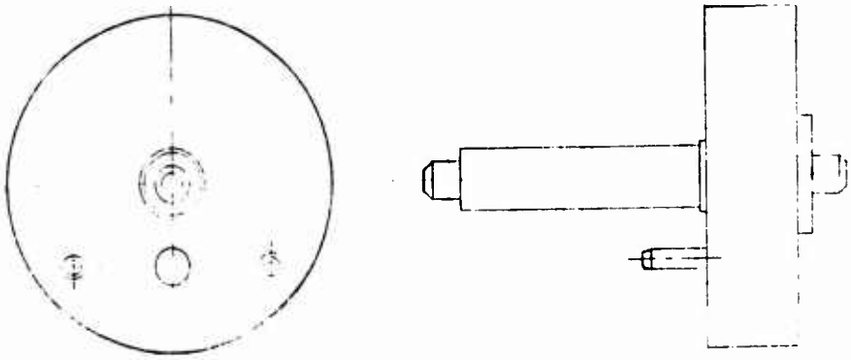

Figure 8. Pallet Lever Contrast

the M125A1 booster, both modular and non-modular designs, considering only the friction between the escapewheel face and pallet pin. * The following analysis considers the same inertia-wheel system considering frictional losses. Frictional torque loss arising simply from the transmission of torque from one gear stage to the next is treated first and then pivot friction is added to account for all frictional losses in the mechanism.

## LOSSES OCCURRING IN TORQUE TRANSMISSION

Torque is transmitted thru the mechanism at three locations. Two of these are gear and pinion meshes while the fourth is the escapewheel-pallet pin contact. All are essentially cam-follower mechanisms and can be analyzed using basic mechanism theory. Qualitatively it can be seen that the presence of friction causes a loss in torque as it is transmitted from one stage to the next. The amount lost is generally described quantitatively in terms of efficiency. If no frictional torque losses occur in a mesh, the efficiency is 100 percent; if losses occur such that no torque is transmitted, the efficiency is 0 percent. The following analysis demonstrates how efficiency is determined given a coefficient of friction, $\mu$, for both gear meshes and the escapement mesh.

### Gear Tooth Losses

The M125A1 booster utilizes clock-type gears whose tooth profiles are essentially circular arcs. The resultant meshing action produces a near rolling motion as the point of contact between gear and pinion crosses the line of centers. Clock gear teeth are known to have pressure angles and gear ratios which vary as the tooth passes thru approach and recess action. Overall, gear efficiency becomes a function of coefficient of friction and contact point position relative to the line of centers. Consider a two gear system (Figure 9) being driven by some power source which produces a "couple" resulting in torque M, applied

---

* Louis P. Farace and Seth D. Shapiro, "Computer Approximation for the Runaway Escapement in Varying Torque Environments: M125A1-M125A1E3 Booster," Frankford Arsenal Report R-2006, May 1971.

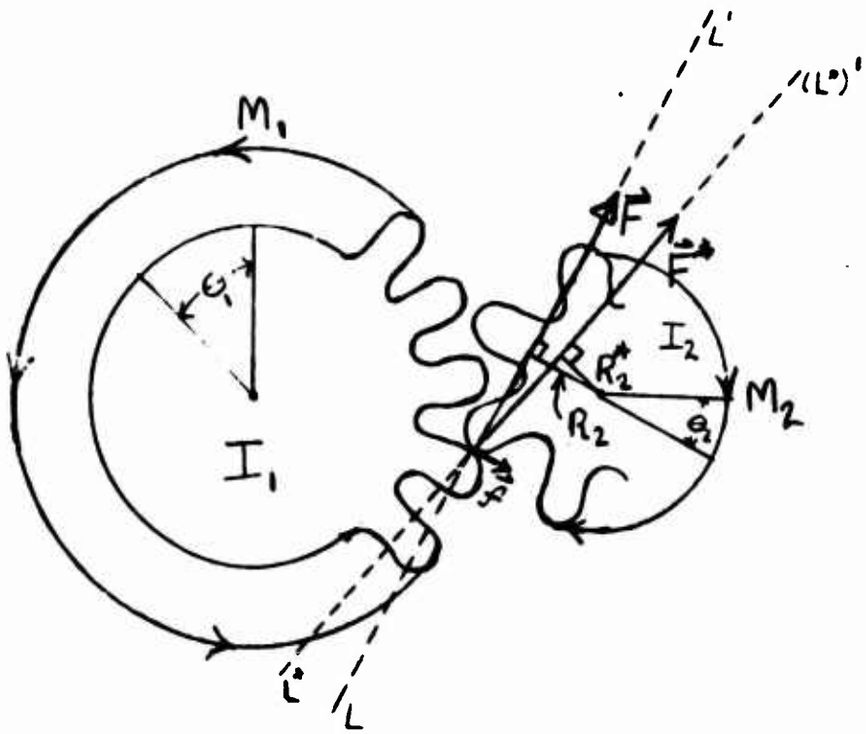


$$\left[I_1 + \eta_{21}\,\eta_{21}^{*}\,I_2\right]\ddot{\theta}_1 = M_1$$

Figure 9. Gears in Contact

on gear 1. The torque transmitted to gear 2 will produce an acceleration $\ddot{\Theta}_2$ on gear 2 given by the equation:

$$\ddot{\Theta}_2 = M_2 / I_2 \qquad (1)$$

where $M_2$ = net torque on gear 2

$I_2$ = inertia of gear 2

In the absence of friction in the bearings of gear 2, the net torque $M_2$ is that torque produced by some net force F* exerted by gear 1 on gear 2 at some radius $R_2^*$. The force F* is the vector sum of the force $\vec{F}$ and the frictional force $\vec{f} = \mu \vec{F}$ which are illustrated in Figure 9. The force $\vec{F}$ acts in a direction along line LL' which passes thru the contact point between gear and pinion and is normal to the contacting surfaces. The magnitude of the moment $F^* R_2^*$ is given by the equation:

$$M_2 = F^* R_2^* = R_p F (\sin \tau \mp \mu \cos \tau) = I_2 \ddot{\Theta}_2 \qquad (2)$$

These parameters are illustrated in Figure 10.

where $R_p$ = position vector locating contact point relative to pinion pivot

$\tau$ = included angle between F and $R_p$.

$\mu$ = coefficient of friction between contacting surfaces

where "-" holds for approach action

"+" holds for recess action

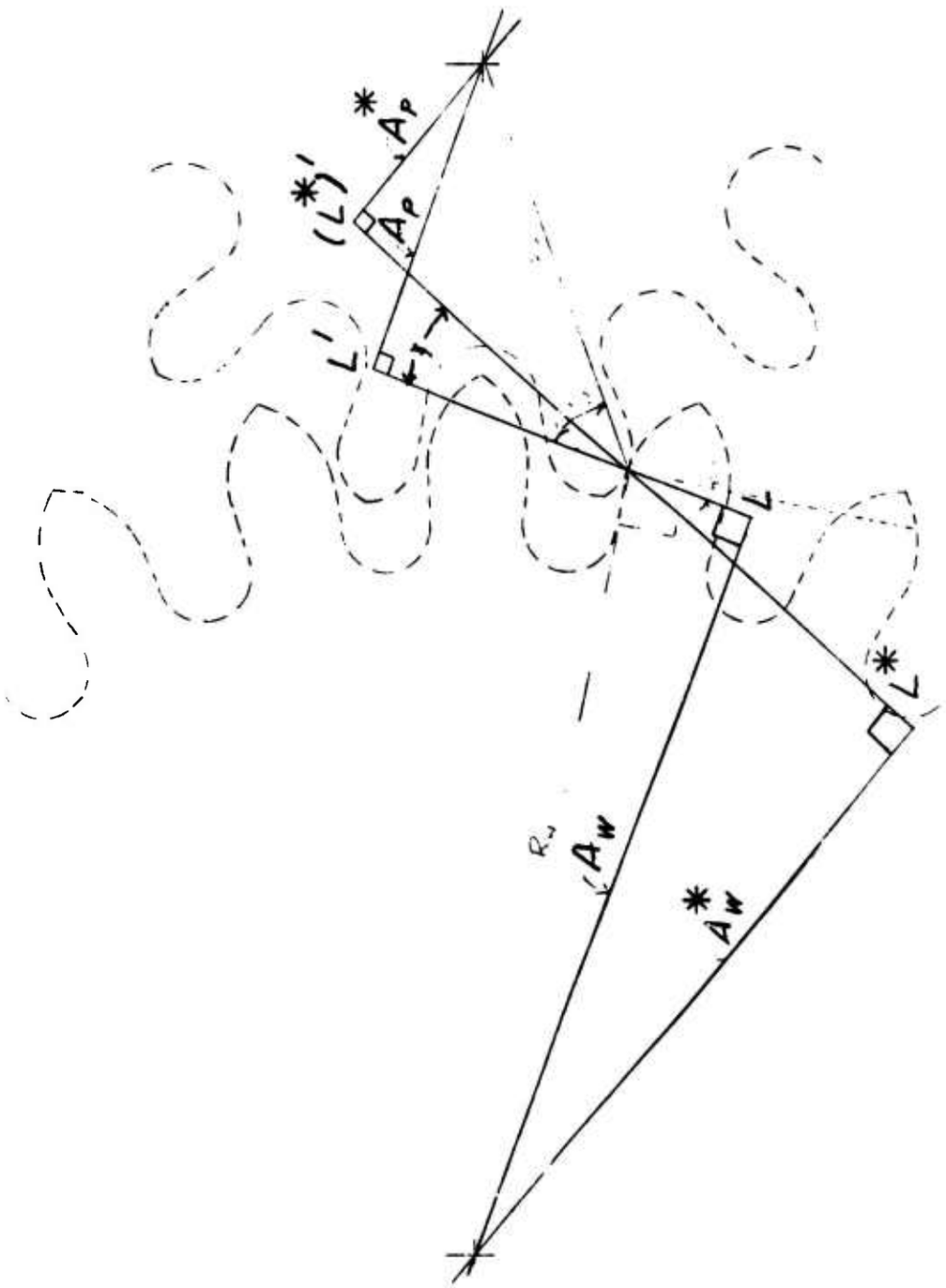


Figure 10. Moment Arms of Force for Gear Contact

Since an equal and opposite reaction to the vector sum $F^*$ is exerted on gear 1, summing moments on gear 1 yields:

$$M_1 - F^* R_1^* = I_1 \ddot{\Theta}_1 \tag{3}$$

where $R^*_1$ = moment arm thru which $F^*$ acts on gear 1.

The magnitude of the reaction torque, $F^* R^*_1$, is as follows:

$$F^* R_1^* = R_w F (\cos\alpha + \mu \sin\alpha) \tag{4}$$

where $R_w$ = position vector locating contact point relative to gear pivot

$\alpha$ = included angle between line of action and normal to $R_w$ at contact point

Combining Equations 2 and 3 and eliminating $F$ we obtain Equation 5.

$$M_1 = I_1 \ddot{\Theta}_1 + R_w \frac{(\cos\alpha + \mu \sin\alpha)}{(\sin\tau \mp \mu \cos\tau)} I_2 \ddot{\Theta}_2 \tag{5}$$

Since $\ddot{\Theta}_2 = \eta \ddot{\Theta}_1$

where $\eta$ = gear ratio for the gear mesh

Substituting into Equation 5 yields:

$$M_1 = \left[ I_1 + \eta_{21} \eta^*_{21} I_2 \right] \ddot{\Theta}_1 \tag{6}$$

$$\text{where } \eta^* = \frac{R_w(\cos\alpha + \mu \sin\alpha)}{R_p(\sin\tau \mp \mu \cos\tau)} \tag{7}$$

"-" holds for approach

"+" holds for recess

The term $\eta_{\text{a}}$ can be computed graphically by taking the ratio of moment arms $A_w$ and $A_p$ illustrated in Figure 10. So that

$$\eta = A_w / A_p \tag{8}$$

$$\text{where } A_w = R_w \cos\alpha$$

$$A_p = R_p \sin\tau$$

The term $\eta^*$ can also be computed graphically by rotating the line of action about the contact point by an angle $\xi = \tan^{-1}\mu$ in the direction of the pinion's pivot. This can be demonstrated by expressing $\mu$ in Equation 3 by

$$\mu = \frac{\sin\xi}{\cos\xi}$$

Thus

$$\eta^* = \frac{R_w\left[\cos\alpha + \left(\frac{\sin\xi}{\cos\xi}\right)\sin\alpha\right]}{R_p\left[\sin\tau \mp \left(\frac{\sin\xi}{\cos\xi}\right)\cos\tau\right]} \tag{9}$$

Multiplying numerator and denominator by $\cos\xi$, the value of $\eta^*$ remains unchanged and can be expressed as,

$$\eta^* = \frac{R_w\left[\cos\alpha\cos\xi + \sin\xi\sin\alpha\right]}{R_p\left[\sin\tau\cos \mp \sin\xi\cos\tau\right]} \tag{10}$$

$$= \frac{R_w}{R_p}\ \frac{\cos(\alpha - \xi)}{\sin(\tau \mp \xi)} = \frac{A_w^*}{A_p^*} \tag{11}$$

Observe that if no friction exists, $\xi = 0$, and $\eta^* = \eta$. The two quantities are also equal when the point of contact between gear and pinion falls on the line of centers. In this case, $\alpha = \frac{\pi}{2} - \tau$, and $\cos\alpha = \sin\tau$. Thus for that particular condition, Equation 8 indicates $\eta^* = R_w/R_p$.

This term $\eta^*$ is sometimes referred to as the torque ratio between gears 2 and 1 since the torque on gear 2 could be computed by dividing the torque on gear 1 by $\eta^*$ in a case where gear one has no inertia.

i.e.

$$M_1 = (M_{out})_1 = F^* R_1^* \tag{12}$$

$$(M_{out})_1 = M_2 = F^* R_2^* \tag{13}$$

where $(M_{out})_1$ = output torque of gear 1

Substituting for $F^*$ from Equation 12.

$$M_2 = M_1 / \eta^* \tag{14}$$

where $\eta^* = R_1^*/R_2^*$

Likewise, for a series of gears, the equation of motion of the system can be given by Equation 15.

$$M_1 = \left[ I_1 + \eta_{21}\eta_{21}^* I_2 + \eta_{31}\eta_{31}^* I_3 + \ldots \eta_{k1}\eta_{k1}^* I_k \right] \ddot{\Theta}_1 \tag{15}$$

where $\eta_{21}$ = gear ratio between gears 2 and 1

$\eta_{31}$ = gear ratio between gears 3 and 1

$\eta_{k1}$ = gear ratio between gears k and 1

$\eta_{21}^*$ = torque ratio between gears 2 and 1

$\eta_{31}^*$ = torque ratio between gears 3 and 1

$\eta_{21}^*$ = torque ratio between gears k and 1

Gear ratios and torque ratios can be determined graphically as previously discussed for each gear mesh. The composite gear ratio can then be computed as follows:

$$\eta_{31} = \eta_{32} \ \eta_{21} \tag{16}$$

$$\eta_{k1} = \eta_{k,k-1} \ \eta_{k-1,1} \tag{17}$$

Likewise, the torque ratios can be computed in the same fashion.

$$\eta^*_{31} = \eta^*_{32} \ \eta^*_{21} \tag{18}$$

$$\eta^*_{k1} = \eta^*_{k,k-1} \ \eta^*_{k-1,1} \tag{19}$$

Since gear meshes are sometimes analyzed in terms of efficiency, the preceeding equations can equivalently be expressed using the relationship:

$$E = \eta/\eta^* \tag{20}$$

Thus the equation of motion of any gear system can be written:

$$M_1 = \left[ I_1 + \sum_{j=2}^{k} \left( \eta_{j1}^2 / E_{j1} \right) I_j \right] \ddot{\Theta}_1 \tag{21}$$

$$M_1 = \left[ I_1 + \sum_{j=2}^{k} \eta_{j1}^2 I_{j1} \right] \ddot{\Theta}_1 \tag{22}$$

Contrasting Equation 21 with 22 one can see that the effect of gear mesh losses is the addition of the "efficiency" term in the effective inertia term. Since $E \leq 1$, the bracketed term, the effective inertia of gear 1, must increase due to frictional losses in the gear teeth.

## Escapement Mesh Losses

### Escapement Efficiency

The frictional losses at the escapewheel pallet pin contact can be quantitatively evaluated in terms of efficiency just as in a gear mesh. The loss arises due to the force exerted by the escapewheel tooth face on the pallet pin. The sliding of the pin along the tooth of the escapewheel results in a resisting frictional force which effects a loss in torque. In the absence of friction, the torque exerted by the escapewheel on the pallet lever is given by

$$G_{p.lev} = G_{s.whl.} / \eta_p \tag{31}$$

where $\eta_p = A_w / A_p$ = speed or gear ratio between escapewheel and pallet lever

These moment arms are illustrated in Figure 11 for entrance engagement. In terms of position vectors to the contact point and torque pressure angles, illustrated in Figure 12:

$$A_w = R_w \cos \alpha \tag{32}$$

$$A_p = R_p \sin \tau \tag{33}$$

$$\eta_p = \frac{R_w \cos \alpha}{R_p \sin \tau} \tag{34}$$

The presence of frictional forces acting along the tooth face in a pin pallet design alters the torque ratio which can be expressed by Equation 35.

$$\eta_p^* = A_w^* / A_p^* \tag{35}$$

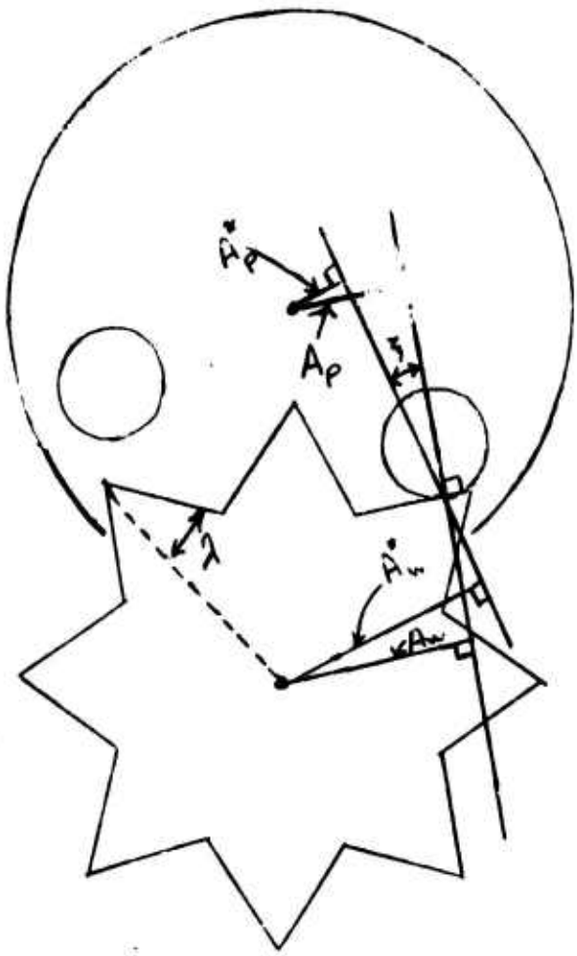


Figure 11. Moment Arms for Escapement Contact

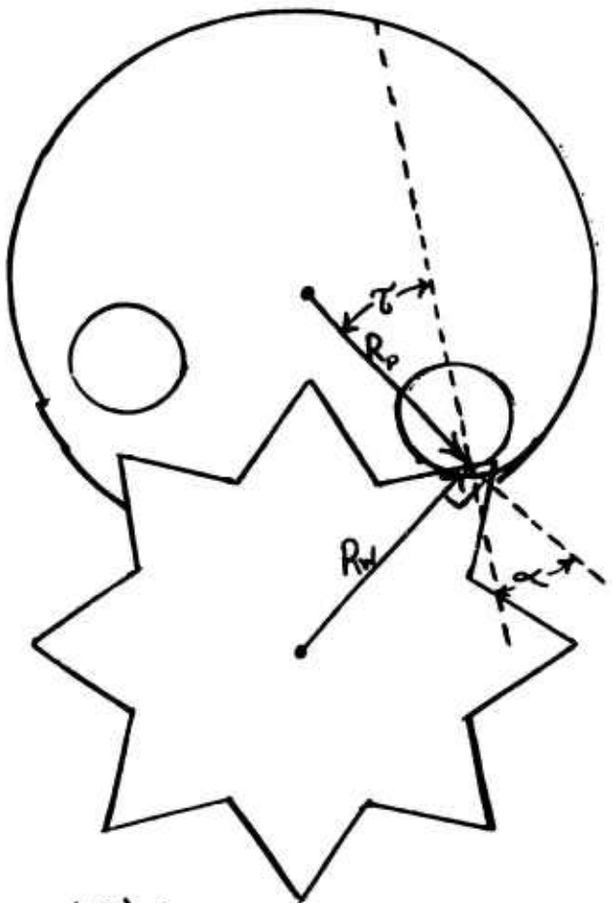


$$\eta = \frac{R_w \cos\alpha}{R_p \sin\gamma} \qquad (18)$$

$$\eta^* = \frac{R_w(\cos\alpha + \mu \sin\alpha)}{R_p(\sin\gamma - \mu\cos\gamma)} \qquad (19)$$

$$E = \eta/\eta^* \qquad (20)$$

Figure 12. Escapement Parameters

These new moment arms are illustrated in Figure 11 for entrance engagement. In terms of position vectors $\vec{R}_w$, $\vec{R}_p$ ; and pressure angles $\tau$ and $\alpha$,

$$\eta_p^* = \frac{R_w (\cos \alpha + \mu \sin \alpha)}{R_p (\sin \tau \mp \mu \cos \tau)} \tag{36}$$

Using double angle formulas and expressing $\mu = \tan \xi$

$$\eta_p^* = \frac{A_w^*}{A_p^*} = \frac{R_w (\cos \alpha \mp \xi)}{R_p (\sin \tau \mp \xi)} \tag{37}$$

N. B. "-" for entrance engagement

"+" for exit engagement

Observe that $\eta_p^* \to \infty$ if $\tau = \xi = \tan^{-1}\mu$ for entrance engagement. Escapement mesh efficiency can then be defined exactly the same as for a gear mesh.

$$E_{esc.} = \eta_p / \eta_p^* \tag{38}$$

$$= \left[ \frac{\sin (\tau \mp \xi)}{\cos (\alpha \mp \xi)} \right] \frac{\cos \alpha}{\sin \tau} \tag{39}$$

$$= \left( A_p^* / A_w^* \right) \left( A_w / A_p \right) \tag{40}$$

When $\xi \to \tau$ for entrance engagement, $E \to 0$. For pin pallet runaway escapements, this angle can be $\cong$ the tooth face angle during entrance engagement as illustrated in Figure 11(angle $\lambda$), dependent on the position of the pallet lever pivot relative to the escapewheel pivot. However, for a verge pallet runaway escapement configuration, this angle is designed into the verge face and is independent of center-to-center distance between the two escapement components. This angle $\tau$ for a verge escapement is illustrated in Figure 13.

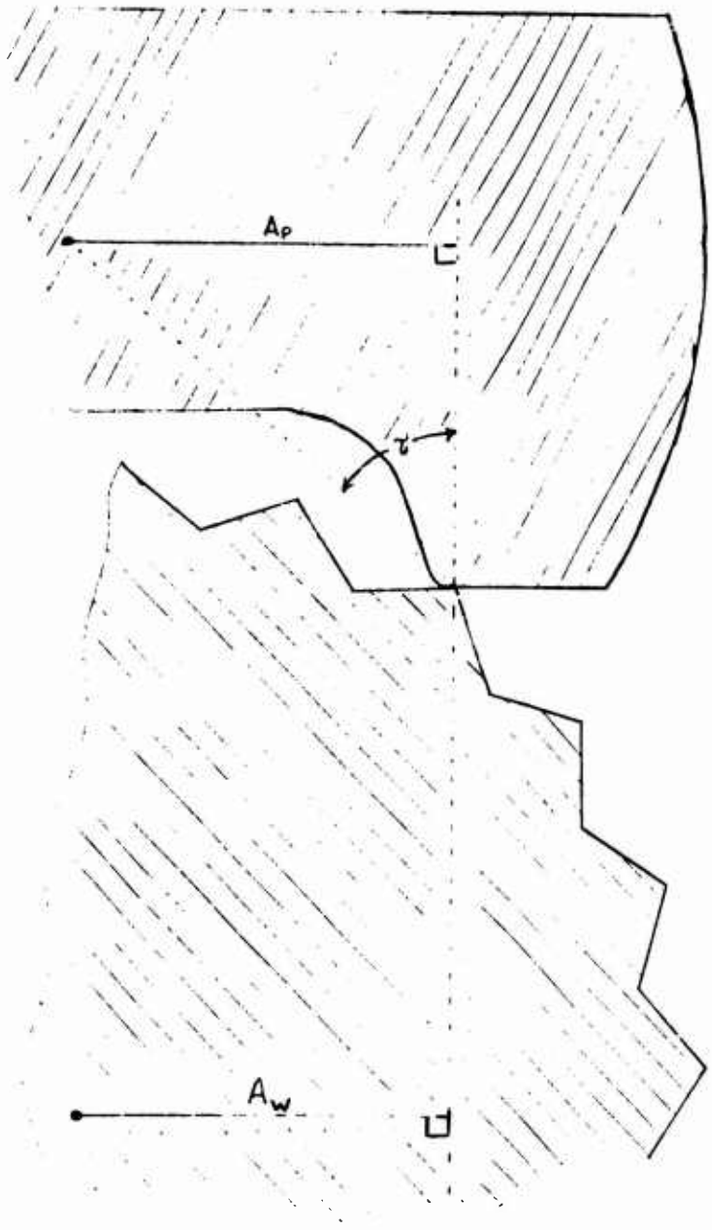


Figure 13. Force Moment Arms for a Verge Escapement

The efficiency value for the escapement mesh is a good measure of how high a value of coefficient of friction a particular escapement design can tolerate before locking due to friction in the escapement mesh. Graphical analysis of runaway escapements to determine efficiency at various points of contact indicate that the most sensitive points of contact from a friction standpoint for a pin pallet runaway escapement occurs when the pallet pin is in the root of the entrance tooth. Angle $\tau$ at this point is at minimum and since $E \rightarrow 0$ when $\mu = \tan\tau$, the efficiency at this point decreases more rapidly as the coefficient of friction increases. In contrast, however, the same situation occurs in the last contact on the entrance face in the verge runaway escapement for the same reason.

## BEARING LOSSES

### General

Consider the same two gear systems as before operating in the presence of bearing losses. Summing moments on gear 2,

$$M_2 = F^* R_2^* - g_2 = I_2 \ddot{\Theta}_2 \tag{41}$$

where $g_2$ = total bearing torque loss in gear stage #2,

Likewise, the equation of motion of gear 1 is,

$$M_1 = M_{input} - g_1 - F^* R_1^* = I_1 \ddot{\Theta}_1 \tag{42}$$

where $g_1$ = total bearing torque loss in gear stage #1,

Combining the two equations and replacing the moment arm ratios by gear ratios and torque ratios defined previously:

$$\left[ I_1 + \eta_{21} \eta_{21}^* I_2 \right] \ddot{\Theta}_1 = M_{input} - (g_1 + \eta_{21}^* g_2) \tag{43}$$

The term in brackets, the effective inertia term, has not changed, however, an effective bearing loss term, the quantity in parenthesis now exists. Notice gear 2's contribution to this effective bearing loss term. The losses at stage 2 are essentially magnified by the $\eta^*_{s1}$ term in contrast with the losses at stage 1. Likewise, for a series of geared elements, using the efficiency concept previously defined:

$$\left[ I_1 + \sum_{j=2}^{k} \frac{\eta_{j1}^2}{E_{j1}} I_j \right] \ddot{\Theta}_1 = M_{input} - \left( g_1 + \sum_{j=2}^{k} \frac{\eta_{j1}}{E_{j1}} g_j \right) \qquad (44)$$

where the "K"th gear is the final gear in the system.

The magnitude of the bearing losses can be computed from standard machine design formulas

Journal Bearing Losses

The M125A1 Modular Version Booster utilizes journal bearings for radial support. For this configuration the friction loss, $g_s$ can be computed by the following equation:

$$g_s = P \rho_p \sin (\tan^{-1} \mu) \qquad (45)$$

$$\approx \mu P \rho_p$$

where $\mu$ = coefficient of friction

$P$ = side load

$\rho_p$ = pivot radius

Thrust Bearing Losses

The gear components are supported parallel to the spin axis in a collar bearing configuration. The frictional loss, $g_t$, can be computed as follows:

$$g_t = \mu P_t \frac{2}{3} \frac{(R_o^3 - R_i^3)}{(R_o^2 - R_i^2)} \qquad (46)$$

where $P_t$ = thrust load

$R_o$ = outer radius of collar bearing

$R_i$ = inner radius of collar bearing

Total Bearing Losses

The total bearing loss at any gear stage is the sum of the two. Thus,

$$g_j = g_s + g_t \tag{47}$$

Sideload losses in this mechanism are generally proportional to $\omega^2$ whereas $g_t$ is not. Insofar as the comparibility of the two losses, it appears that at about 500 rpm the two terms $g_s$ and $g_t$ are approximately equal if thrustload is produced solely by the gravitational weight of the gear component.

## ADDITIONAL FRICTIONAL LOSSES PRESENT IN THE MECHANISM

The equations discussed so far apply to any time delay mechanism utilizing a runaway escapement. Frictional losses in general come about from two sources - bearings and meshes. However, in some devices, additional losses are sometimes introduced which are peculiar to those devices only. An example of such a loss is that induced by the rotor locking system in the M125A1 Modular Booster. This system consists of a spring loaded pin which pops into a hole in the upper movement plate when the rotor reaches the armed position. Throughout the arming cycle it drags along the underside of the movement plate producing a frictional torque which must be accounted for in the math model apart from those losses already considered. In addition, the bias of the pin produces an additional thrust bearing load on the rotor thrust bearing yielding additional frictional losses.

Once the magnitude of these frictional torque losses are computed, they can be lumped with the other losses in Equation 47. Note in this case that this is a frictional loss which is not spin dependent and hence, becomes insignificant at high spin levels but is significant at low levels.

## SUMMARY OF MATH MODEL

Figure 14 illustrates the observed velocity of the escapewheel member of a runaway escapement vs. time for two half oscillations of the lever.

Since the remainder of the gear train is geared to the escapewheel their motion must be coincident with that of the escapewheel except the angular velocity would be scaled down by the respective gear ratio between that gear and the escapewheel. The equations of motion, as derived previously in this report are as follows:

(1) for engagement portion of motion (escapewheel directly driving pallet lever) represented by the gradual slopes in Figure 14.

$$\left[ I_1 + \left( \sum_{j=2}^{k} \frac{\eta_{j1}^2 I_j}{E_{j1}} \right) + \frac{\eta_{L1}^2}{E_{L1}} I_L \right] \ddot{\Theta}_1 = M_{input} - \left( g_1 + \sum_{j=2}^{k} \frac{\eta_{j1}}{E_{j1}} g_j \right) - \frac{\eta_{L1}}{E_{L1}} g_L$$

where $I_1$ = Inertia of first gear

$I_j$ = Inertia of gear "i"

$I_L$ = Inertia of pallet lever

$I_k$ = Inertia of escapewheel

$\eta_{j1}$ = Gear ratio between gears 1 and "i"

$\eta_{L1}$ = Gear ratio between gears 1 and pallet lever

$E_{j1}$ = composite gear efficiency between gears 1 and "i"

$E_{L1}$ = composite mesh efficiency between pallet lever and gear

$\ddot{\Theta}_1$ = ang. acceleration of gear 1

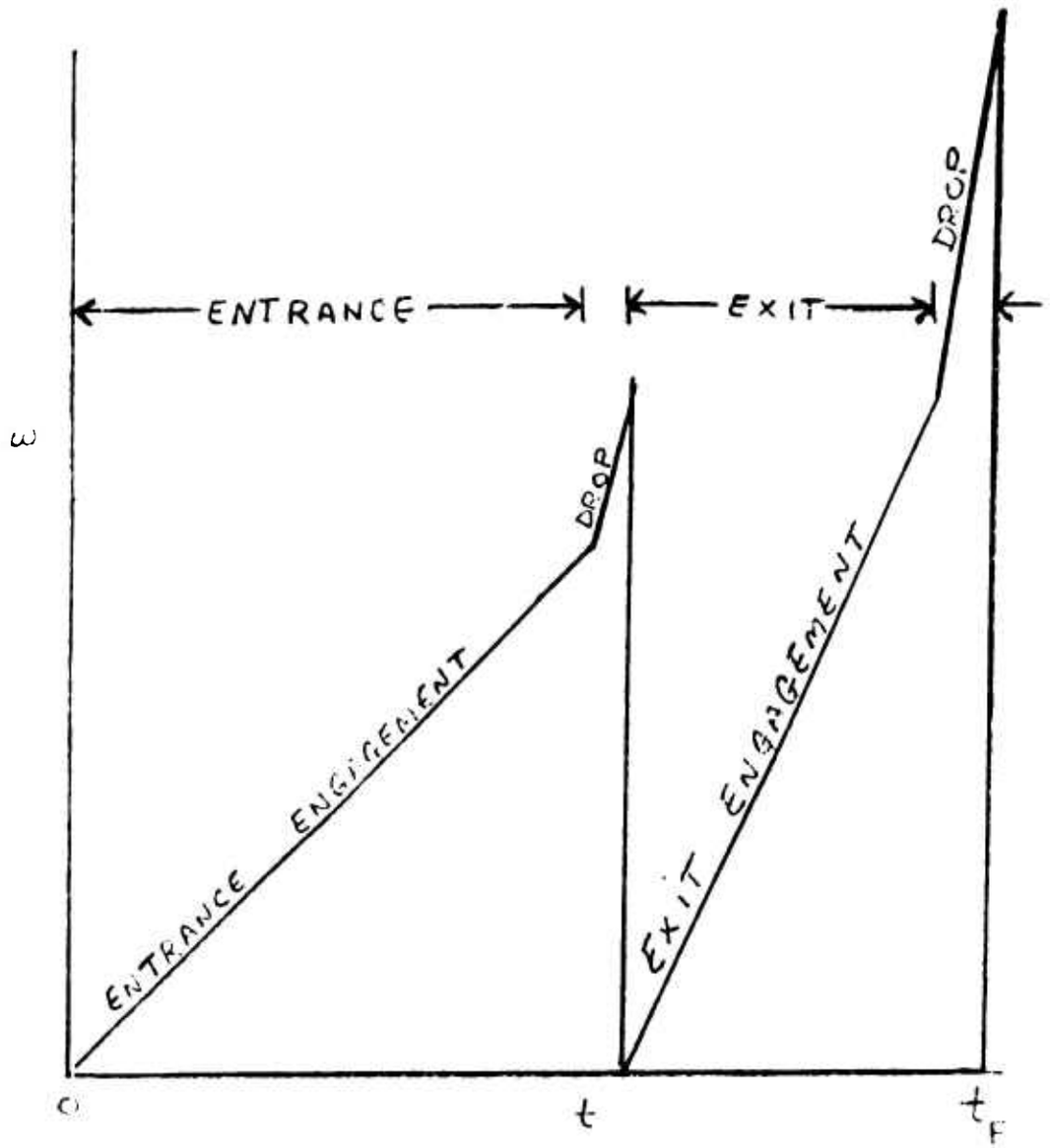


$$\int_0^{t_F} \omega \, dt = \frac{\pi}{108}$$

Figure 14. Angular Velocity of Main Gear vs Time Inertia Wheel Approach

$M_{in}$ = input torque on gear 1

$g_1$ = bearing loss at gear 1

$g_j$ = bearing loss at gear "i"

$g_L$ = bearing loss at pallet lever

(2) For drop portions of motion (escapewheel and pallet not linked) represented by the increased slope portions of Figure 14, the equation of motion is the same but $I_L$ and $g_L$ are equal to zero.

### Comments

1. The extremely difficult problem of describing the motion of the system when the wheel impacts the pallet pin (once per half cycle) has not been addressed here and is not within the scope of this report. This phase (impact) determines the boundary values for the equations of motion described here.

2. As an approximation, one can consider that this impact causes the escapewheel and lever's angular velocity to drop to zero. High speed films of the high inertia lever described herein show this impact actually driving the escapewheel backwards. This need not be the case with all runaway escapements.

## EQUATION OF MOTION APPLIED TO M125A1 MODULAR BOOSTER

The M125A1 Modular Booster consists of the rotor gear, one gear and pinion assembly, an escapewheel and pinion assembly, and a pallet lever.

Thus,

$I_1$ = inertia of rotor gear

$I_2$ = inertia of the gear pinion assembly

$I_3$ = inertia of the escapewheel and pinion assembly

$I_p$ = inertia of pallet lever assembly

The equation of motion becomes:

$$\left[ I_1 + \frac{n_{21}^2}{E_{21}} I_2 + \frac{n_{31}^2 I_{31}}{E_{31}} \quad \frac{\eta_{p_1} I_p}{E_{p_1}} \right] \ddot{\Theta}_1 = M_{input} - \left( g_1 + \frac{n_{21} g_2}{E_{21}} + \frac{n_{31} g_3}{E_{31}} + \frac{n_{p_1} g_p}{E_{p_1}} \right)$$

Gear ratios $n_{21}$ and $n_{31}$ are 6 and 18 respectively. The quantity $n_{21}$ can also be written as the product $n_{31} n_p$. The efficiency $E_{p1}$ can be written similarly as the product $E_{31} E_p$. Substitution into the above equation yields:

$$\left[ I_1 + \frac{(6)^2}{E_{21}} I_2 + \frac{(18)^2}{E_{31}} I_3 + \frac{(18)^2 \eta_p^2}{E_p E_{31}} I_{pL} \right] \quad X$$

$$\ddot{\Theta}_1 = M_{input} - \left( g_r + \frac{6 g_2}{E_{21}} + \frac{18 g_3}{E_{31}} + \frac{18 \eta_p g_p}{E_{31} E_p} \right)$$

i.e.

$$\left[ I_1 + \frac{36}{E_{21}} I_2 + \frac{324}{E_{31}} I_3 + \frac{324 \eta_p^2}{E_{31} E_p} I_{pL} \right] X$$

$$\ddot{\Theta}_1 = M_{input} - \left( g_1 + \frac{6 g_2}{E_{21}} + \frac{18 g_3}{E_{31}} + \frac{18 \eta_p g_p}{E_{31} E_p} \right)$$

Note the following about the above equations insofar as evaluation of the remaining terms:

1. The efficiency terms ("$E_{ij}$" terms) have values $0 < E_{ij} < 1.0$
2. $E_{31}$ will always be $\leq E_{21}$. The product $E_p E_{31}$ will always be $\leq E_{31}$.

3. The linkage ratio, $\eta_p$, for the two runaway escapement designs discussed herein (see next section for numerical values) are >1.0.

4. $I_1$ and $g_1$, the rotor's inertia and frictional bearing loss respectively are much larger in magnitude than the other gear train component's inertia and bearing loss because of the large physical size of the rotor gear assembly. However, both have coefficients in the equation equal to 1.0 in contrast with the lever's inertia which has a magnifying coefficient of over 400 and the lever's bearing loss which has a magnifying coefficient greater than 30.

One can readily see that the final terms in brackets are the most heavily weighted and by far the most important. In general, the lever's inertia is the controlling inertia in the effective inertia term while the lever's bearing loss is the most predominant term in the effective bearing loss term. The linkage ratio, $\eta_p$; linkage efficiency, Ep; and escapewheel to rotor gear ratio, $E_{31}$; are also of importance because of their appearance in these final terms. Unfortunately, improving the frictional loss situation by reducing the escapewheel to rotor gear ratio also results in a corresponding loss in the number of oscillations the escapement will make for a given rotation of the rotor. A more fruitful area for improvement, then, is in the escapement.

## QUANTITATIVE COMPARISON OF REDESIGN AND ORIGINAL DESIGN

A quantitative comparison can be made between the frictional torque at the pallet lever before and after the subject design changes. These vary with coefficient of friction and spin rate of the projectile considered. The following equation assumes that any loading on the pallet's journals produced by the escapewheel is negligible in comparison with the centrifugal force loading on the lever:

$$g_{p.L} = g_{s.p.L.} + g_{t.p.L.}$$

$$= m_{p.L.}\ \omega^2\ R_{p.L.}\ \mu\ \rho_{p.L.} + m_{p.L.}\ a\ \mu\ \frac{2}{3}\left(\frac{R^3_{o.p.} - R^3_{i.p.}}{R^2_{o.p.} - R^2_{i.p.}}\right)$$

$$= m_{p.L.}\ \mu\left[\omega^2\ R_{p.L.}\ \rho_{p.L.} + \frac{2a}{3}\left(\frac{R^3_{o.p.} - R^3_{i.p.}}{R^2_{o.p.} - R^2_{i.p.}}\right)\right]$$

where $g_{p.L.}$ = Frictional torque loss in bearings

$g_{s.p.L.}$ = Frictional torque at this stage due to sideload reaction forces

$g_{t.p.L.}$ = Frictional torque at this stage due to thrust load forces

$m_{p.L.}$ = Mass of pallet lever

$R_{p.L.}$ = Radial location of pallet lever from projectile spin axis

$\mu$ = Coefficient of friction in lever's bearings

$\rho_{p.L.}$ = Journal radius of pallet lever

$a$ = Acceleration environment (one "g" for normal laboratory testing)

$R_{o.p.}$ = Outer radius of pallet lever's collar bearing (lower collar bearing for typical laboratory testing)

$R_{i.p.}$ = Inner radius of collar bearing

$\omega$ = Spin rate of projectile

Since the rotor torque is proportional to $\omega^2$, $g_{p.L.}$ will be expressed similarly as follows:

$$g_{p.L.} = \mu m_{p.L.} \omega^2 \left[ R_{p.L.} \rho_{p.L.} + \frac{2a}{3\omega^2} \left( \frac{R_{o.p.}^3 - R_{i.p.}^3}{R_{o.p.}^2 - R_{i.p.}^2} \right) \right]$$

Figure 15 indicates the contrast in the friction torque present in the bearings of the pallet lever vs spin rate. The reduction is approximately 51 percent.

A quantitative comparison can also be made between the torque transmisted by the escapewheel to the pallet lever by contrasting the linkage ratios in the two escapements.

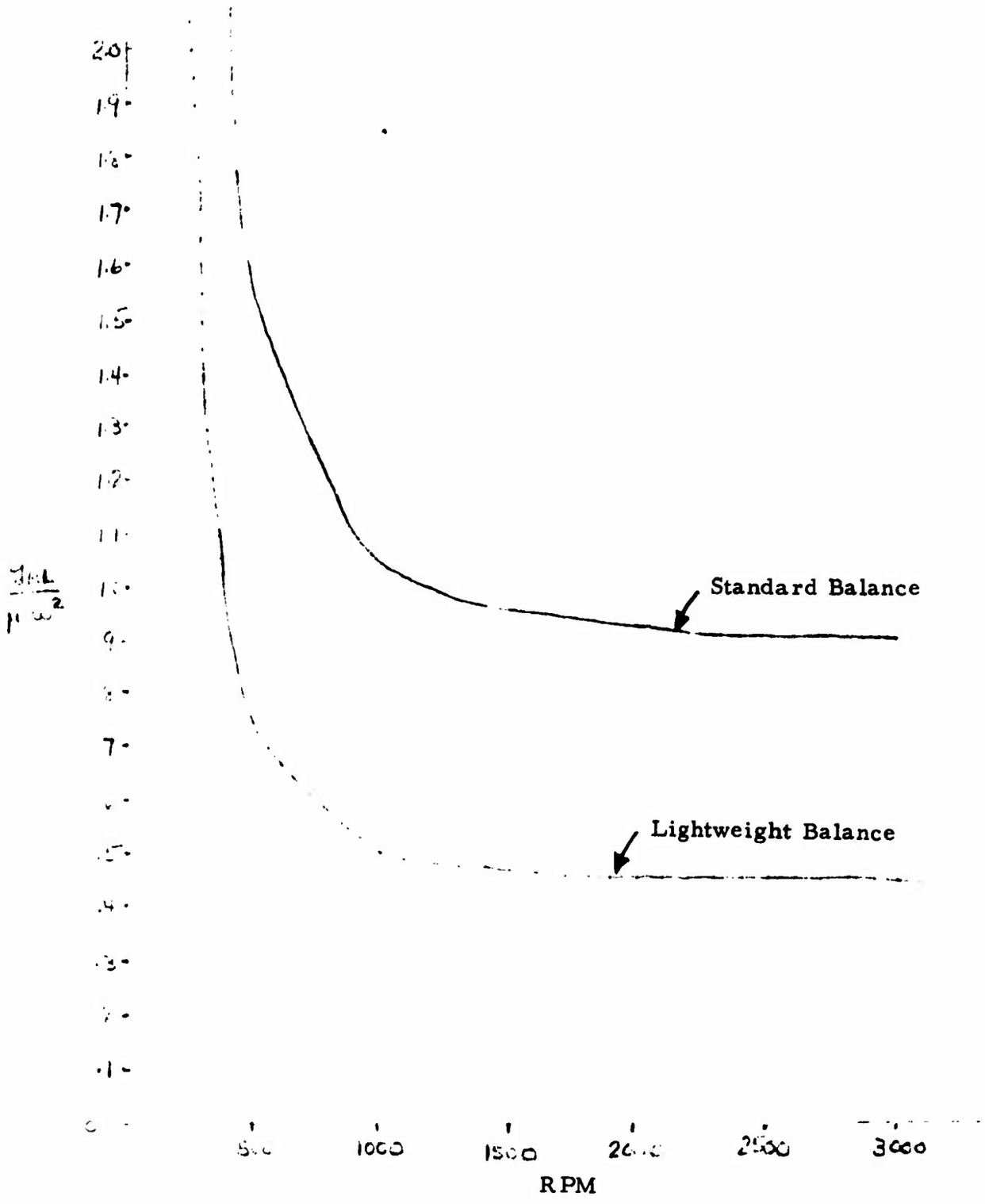


Figure 15. Frictional Torque in Lever Bearings vs Spin Rate

The minimum angle of oscillation of the lever for both escapements at nominal dimension is approximately 8°. The following is a comparison of the linkage ratios and efficiencies of the two designs for various points of contact. Keep in mind that the torque transmitted from the escapewheel to the pallet is inversely proportional to the linkage ratio, i.e., for no friction:

$$M_{p.L.} = M_{es\ whl} \ / \eta_p$$

where $M_{p.L.}$ = torque transmitted to pallet lever

$M_{es\ whl}$ = net torque on escapewheel

$\eta_p$ = linkage ratio

Since the objective here is to increase the torque to the lever, the lower the linkage ratio the better. Similarly we wish to maximize the efficiency of this torque transmission since when friction is considered.

$$M_{p.L.} = E_p M_{es\ whl} \ / \eta_p$$

Thus the higher the efficiency, the more torque transmitted to the lever.

The escapement positions considered first are those which the escapement MUST pass through. The nature of runaway escapement action is such that the range of actual escapement positions is determined by dynamic considerations. Theoretically the pallet pin can swing into the root of the tooth and travel along the full face of the escapewheel tooth. Since the passage of the tooth along the escapement wheel face indexes the opposite pin in the well of some adjacent tooth, a minimum angle of oscillation is guaranteed and hence a given

range of escapement positions is established. These positions are considered first:

TABLE II.
Linkage Ratios and Mesh Efficiency Values

Entrance Engagement

| | Original Escapement | | Modified Escapement | |
|---|---|---|---|---|
| Pallet Position | Linkage Ratio | Efficiency at $\mu$ = .2 | Linkage Ratio | Efficiency at $\mu$ = .2 |
| First Contact | 1.9193 | .5438 | 1.4186 | .6545 |
| +1° | 1.9342 | .5516 | 1.4524 | .6595 |
| +2° | 1.9484 | .5592 | 1.4850 | .6645 |
| +3° | 1.9619 | .5667 | 1.5167 | .6693 |
| +4° | 1.9748 | .5741 | 1.5474 | .6739 |
| +5° | 1.9870 | .5812 | 1.5772 | .6784 |
| +6° | 1.9986 | .5882 | 1.6061 | .6828 |
| +7° | 2.0098 | .5951 | 1.6342 | .6871 |
| +8° | 2.0204 | .6018 | 1.6615 | .6914 |
| Last Contact | 2.0278 | .6066 | 1.6624 | .6915 |

Exit Engagement

| | Original Escapement | | Modified Escapement | |
|---|---|---|---|---|
| Pallet Position | Linkage Ratio | Efficiency at $\mu$ = .2 | Linkage Ratio | Efficiency at $\mu$ = .2 |
| First Contact | 1.3944 | .7195 | 1.5235 | .6980 |
| +1° | 1.4732 | .7104 | 1.5961 | .6963 |
| +2° | 1.5575 | .7008 | 1.6715 | .6942 |
| +3° | 1.6477 | .6904 | 1.7502 | .6917 |
| +4° | 1.7444 | .6793 | 1.8324 | .6888 |
| +5° | 1.8483 | .6675 | 1.9184 | .6855 |
| +6° | 1.9603 | .6548 | 2.0086 | .6818 |
| +7° | 2.0811 | .6411 | 2.1033 | .6776 |
| +8° | 2.2118 | .6264 | 2.2030 | .6730 |
| Last Contact | 2.3140 | .6149 | 2.2064 | .6728 |

The above figures indicate that for $\mu$ = .2, approximately 50 percent more torque is transmitted to the pallet lever during entrance

engagement and approximately 3 percent less torque during exit engagement than with the original design. The improvement in the entrance impulse is especially significant insofar as the 2000 rpm acceptance spin test since the angular acceleration experienced by the booster tends to swing the escapement into entrance engagement thus establishing a preferred starting position or range thereof. It is here that the possibility of contact between the pin and tooth in the root comes into play. Compare the following efficiencies and linkage ratios for this position vs coefficient of friction:

TABLE III.
Efficiency Comparison at Root of Entrance Tooth

| | Original Escapement | | Modified Escapement | |
|---|---|---|---|---|
| Coefficient of Friction | Linkage Ratio | Efficiency | Linkage Ratio | Efficiency |
| = 0.0 | 1.89 | 1.000 | 1.11 | 1.0000 |
| 0.1 | 1.89 | .721 | 1.11 | .7734 |
| 0.2 | 1.89 | .474 | 1.11 | .6096 |
| 0.3 | 1.89 | .258 | 1.11 | .4858 |
| 0.4 | 1.89 | .063 | 1.11 | .3888 |
| 0.435 | 1.89 | .000 | 1.11 | .3597 |

These yield the following percentage increases in transmitted torque vs. coefficient of friction over the original escapement design:

| Coefficient of Friction ($\mu$) | % Torque Increase |
|---|---|
| .1 | 70.3 |
| .2 | 82.6 |
| .3 | 320.6 |
| .4 | 1050.8 |

As can be seen from the above figures, the modified escapement is more capable of operating in high friction environments, especially insofar as starting.

The combination escapement - pallet configuration change, then, increases the overall torque transmitted to the lever and decreases the frictional torque present in the lever's bearings. Thus the net torque on the pallet lever increases. The magnitude depends on what coefficients of friction actually exist between 1) the pallet pin and escapewheel tooth face and 2) the lever's journal staff and movement plate hole sidewall, and 3) the lever's lower thrust bearing and movement plate surface. If the final frequency of the two escapements remain the same, one can approximate the dynamic net torque increase by taking the ratio of the inertia of the two pallet levers. This indicates an overall increase in net torque on the lever (transmitted torque less frictional bearing torque) of 43.75 percent.

## Escapewheel Inertia

The larger diameter escapewheel (.384 nominal) used in the modified design is higher in inertia than the pointed tooth escapewheel in the original design (.368 diameter nominal). Estimated inertia value for the larger wheel is $.28 \times 10^{-6}$ sl. in.$^2$ vs. $.168 \times 10^{-6}$ sl. in.$^2$ for the smaller. In contrast with their respective pallet lever inertias, they are small (10 x smaller for original wheel, 8.2 x smaller for the larger wheel). Insofar as their contribution to the effective inertia of the entire gear train during the engagement portions of escapement motion, their effect in both cases is insignificant. However, during the "drop" phases of escapement motion, the gear train is running free of the pallet lever. In this case, the escapewheel inertia is the predominant contributor to the effective inertia term. One would, therefore, predict a slower angular acceleration of the modified system during "drop" than with the original system. These portions of the running cycle are generally rather small in comparison with the engagement portion of the running cycle and should make little difference in arming time.

## Pallet Lever Inertia

The new configuration of the pallet lever results in an increase in the lever's radius of gyration. The area of this shape is .0909 in.$^2$, 12.3 percent less than that of the round lever shape it replaces (.021 in.$^2$). The area moment of inertia, however, increases by 287.73 percent from .001658 in.$^4$ to .004771 in.$^4$

Since

$$k = \sqrt{I/M}$$

where $k$ = radius of gyration

$I$ = inertia

$M$ = mass

the radius of gyration increases by 79.8 percent from .1274 in. to .2291 in.

The extended lever is only .051 in. thick, 50 percent of the thickness of the round pallet lever. The resultant increase in polar moment of inertia, then, is approximately 44 percent. The overall weight of the lever, however, decreased 46 percent.

The Inertia of the modified lever is approximately $2.3 \times 10^{-6}$ sl. in.$^2$ vs. $1.69 \times 10^{-6}$ sl. in.$^2$ for the original round pallet lever. This higher inertia was required to maintain the required time delay (turns) since the new escapement geometry transmits more torque to the lever, inherently tending to speed up the mechanism. The resultant combination actually produced a time delay of approximately 31.95 turns in contrast with the 30 turn arming delay of the original design. The modified units for the arming distance test, however, utilized escapewheels made toward the higher side of the permissible range of escapewheel diameters which tend to produce a slightly slower running unit.

## MASS PRODUCTION OF NEW ESCAPEMENT

The escapement changes described in this report were EO'd into the TDP on a non-obsolescence basis. Of three contractors who are presently producing this modified design, two are purchasing the pallet lever and drilling and pallet pin holes while the third is piercing these holes while blanking the lever.

In general, dropout at the 2000 rpm acceptance spin test has been dramatically reduced. One contractor who was using a teflon dry film lubricant to reduce the fallout from this test to an acceptable level found that this lubricant was no longer needed when these escapement changes were implemented into his contract. Another contractor claims his fallout to be virtually non-existant. It is apparant that a reduction in cost should ultimately result from this decrease in scrap rate. It is also expected that reliability in field usage should improve, especially in low spin weapons.

## SUMMARY

Design modifications were made to the M125A1 modular booster in the escapement area for the purpose of improving the low spin operating capability of the device. Prototypes of three different versions of the improved design were fabricated and tested both ballistically and in the laboratory. These prototypes performed well in all cases. The final version is such that it is suitable for fabrication in large quantities using standard mass production techniques.

These design changes are now reflected in the M125A1 TDP. Mass production of this modified design has demonstrated that all design objectives have been met. Fall-out rate at 2000 rpm has been significantly decreased. No duds were observed throughout initial prototype testing of nearly five hundred rounds.

## RECOMMENDATIONS

The type design changes made here to the M125A1 can, in theory, be made to any runaway escapement device, especially those experiencing a reliability problem. Exercising the math model developed to describe frictional losses can be used to reduce friction and increase operational efficiency. In this respect it can be seen that the Modular M125A1 can be further improved by reducing the diameter of the journal bearings, lightening the gear train members, and developing some rotor lock system which yields lower frictional losses. It is also conceivable that some alternate rotor design can be established which would deliver the same output torque but be lighter in weight yielding lower frictional losses.

Unless any of these changes are found to decrease production costs, at this point they appear superfluous. The present design can operate at 1000 rpm whereas the acceptance requirement is 2000 rpm. The lowest ballistic spin experienced for current weapons which use the M125A1 Booster is 2950 rpm. Thus, while further improvement is possible, it does not appear necessary for present applications. However, it should be observed that the framework for further improvement exists should future requirements arise for a device to be operable in very low spin or torque environments.